Title

JASON: A DIGITAL COMPUTER PROGRAM FOR THE NUMERICAL SOLUTION OF THE LINEAR POISSON EQUATION v (kvo) +p =0

Authors

Sackett, S.
Healey, R.

Publication Date

1969-02-01

UCRL-18721

JASON - A DIGITAL COMPUTER PROGRAM FOR THE NUMERICAL SOLUTION OF THE LINEAR POISSON EQUATION

$$\nabla \cdot (\kappa \nabla \phi) + \rho = 0$$

S. Sackett and R. Healey

February 1969

LRL
LAWRENCE RADIATION LABORATORY
UNIVERSITY of CALIFORNIA BERKELEY

UCRL-18721

DISCLAIMER

C. 2

UCRL-18721
Mathematics and
Computing UC-32
TID-4500 (54th Ed.)

UNIVERSITY OF CALIFORNIA

Lawrence Radiation Laboratory
Berkeley, California

AEC Contract No. W-7405-eng-48

JASON - A DIGITAL COMPUTER PROGRAM FOR THE NUMERICAL SOLUTION OF THE LINEAR POISSON EQUATION

$$\underline{\nabla} \cdot (\underset{\sim}{\kappa}\, \underline{\nabla} \phi) + \rho = 0$$

S. Sackett and R. Healey

February 1969

Printed in the United States of America
Available from
Clearinghouse for Federal Scientific and Technical Information
National Bureau of Standards, U. S. Department of Commerce
Springfield, Virginia 22151
Price: Printed Copy $3.00; Microfiche $0.65

CONTENTS

UCRL-18721

JASON - A DIGITAL COMPUTER PROGRAM FOR THE NUMERICAL SOLUTION OF THE LINEAR POISSON EQUATION

S. Sackett
R. Healey

Lawrence Radiation Laboratory
University of California
Berkeley, California

February 1969

ABSTRACT

This paper describes the development of a high-speed computer program for the solution of the Linear Poisson Equation

$$\underline{\nabla} \cdot (\underset{\sim}{\kappa} \underline{\nabla} \phi) + \rho = 0,$$

where ϕ and ρ are scalar functions of two independent variables, and $\underset{\sim}{\kappa}$ is a second rank tensor whose components are functions of two independent variables. The mathematical model is given in detail. Examples showing the application of the program to the solution of problems in electrostatics demonstrates its speed and accuracy.

Outstanding characteristics of JASON, in addition to speed, are the following:

(1) usage for both cylindrically symmetric systems and for two-dimensional Cartesian systems,

(2) completely general boundary conditions (Neumann, Dirichlet),

(3) generalized quadrilateral mesh,

(4) utilization of algorithms which ensure continuity of ϕ across mesh lines,

(5) use of block iterative methods for solution of the equations,

(6) ease and simplicity of input,

(7) consideration of nonhomogeneous, anisotropic media through use of the tensor $\underset{\sim}{K}$.

MATHEMATICAL MODEL

In this section, a mathematical model for numerical solution of the linear Poisson equation

$$\underline{\nabla}\cdot(\underset{\sim}{K}\,\underline{\nabla}\phi) + \rho = 0 \tag{1}$$

is constructed; ϕ and ρ are scalar functions of two independent variables and $\underset{\sim}{K}$ is a second-rank tensor whose components are functions of two independent variables. The development is limited to systems possessing cylindrical symmetry. In addition, it is assumed that the tensor, $\underset{\sim}{K}$, is diagonal in the coordinate system chosen:

$$\phi = \phi(r,z) \quad ; \quad \rho = \rho(r,z) \quad ; \quad \underset{\sim}{K} = \begin{bmatrix} K_r(r,z) & 0 \\ 0 & K_z(r,z) \end{bmatrix} . \tag{1a}$$

esu/cm³

We will also show how the equations derived here for the cylindrical case can be applied to two-dimensional Cartesian systems. The development given here follows the work of Zienkiewicz [1].

For systems with cylindrical symmetry, equation (1) can be written as

$$\frac{\partial}{\partial r}\left(K_r \frac{\partial\phi}{\partial r}\right) + \frac{K}{r} r \frac{\partial\phi}{\partial r} + \frac{\partial}{\partial z}\left(K_z \frac{\partial\phi}{\partial z}\right) + \rho(r,z) = 0; \tag{2}$$

this is the Euler-Lagrange equation associated with the functional

$$I(\phi) = \int_R \frac{r}{2}\left[K_r\left(\frac{\partial\phi}{\partial r}\right)^2 + K_z\left(\frac{\partial\phi}{\partial z}\right)^2 - 2\rho\phi\right] drdz + \int_C qr\phi\, ds, \tag{3}$$

where R is open region of two-dimensional space, C is one or more differentiable curves bounding R, and ϕ is assumed to be of class C^1 on $R \cup C$.

Applying the variational principle, we find that any function, ϕ, which renders (3) stationary in R, satisfies (2) in R subject to the natural boundary condition

$$(\underset{\sim}{\kappa}\underline{\nabla}\phi)_n + q = 0 \qquad (4)$$

on C, where n denotes the outward normal component on the contour C [2]. Note that the second integral in (3) is identically zero whenever r is zero (since ϕ is C^1). This ensures that $(\underset{\sim}{\kappa}\underline{\nabla}\phi)_n = 0$ whenever r is zero, a necessary condition for cylindrical symmetry.

To construct a set of difference equations approximating (2) in R, we use the "finite element method" [1]. We first divide the region, R, into a finite number of subregions, or elements, R^e, e = 1,···,N , such that

$$\bigcup_{e=1}^{N} R^e = R,$$

$$R^e \cap R^f = \emptyset \quad ; \quad e,f = 1,\cdots,N \quad , \quad e\neq f, \qquad (5)$$

and such that the contour C is approximated by an exclusive union of sides of the R^e, e = 1,...,N. For our purposes, we take the elements to be polygons of four nodes (corners):

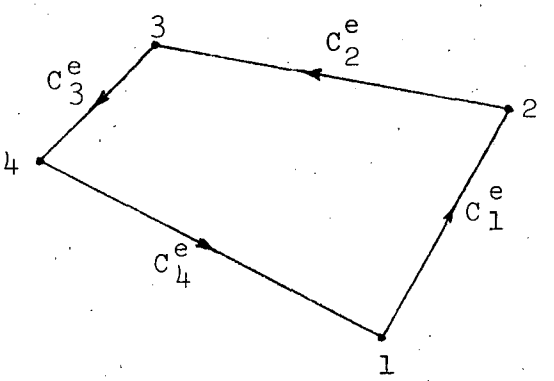

It is clear that a construction of such elements can be easily made to satisfy conditions (5).

Assuming that within each element the variation of ϕ is prescribed by the values of ϕ associated with the nodes of the element, we have

$$\phi^e(r,z) = [N]^e \{\phi\}^e = N_1^e\phi_1 + N_2^e\phi_2 + N_3^e\phi_3 + N_4^e\phi_4, \qquad (6)$$

in which the matrix $[N]^e$ involves suitable functions of coordinates.

The condition for ϕ to render $I(\phi)$ stationary is that

$$\frac{\partial I(\phi)}{\partial \phi} = 0.$$

For a given set of values of $\{\phi\} = \sum_{e=1}^{N} \{\phi\}^e$, therefore, (3) can be rendered approximately stationary by satisfying the set of equations

$$\frac{\partial I(\phi)}{\partial \phi_s} = 0 \quad ; \quad s = 1,\cdots,m, \qquad (7)$$

where m is the total number of distinct elements in the set $\{\phi\}$, i.e., the number of distinct nodes in the region $R = \bigcup_{e=1}^{N} R_e$.

Let $I(\phi)^e$ be the contribution of an element, e, to the total integral $I(\phi)$. Then we have

$$I(\phi) = \sum_{e=1}^{N} I(\phi)^e, \qquad (8)$$

provided none of the $I(\phi)^e$ are infinite. Since $I(\phi)$, and consequently $I(\phi)^e$, depends only on the first derivative of ϕ, this condition will be satisfied if ϕ is of class C^1 on R and C. This was one of our assumptions in applying the variational principle. A condition on the matrix $[N]^e$ is, therefore, that it be constructed of functions which

are of class C^1 on R^e and C^e, C^e denoting the boundary of the element R^e.

Using equations (3), (6), and (8), we have the following relation:

$$\frac{\partial I(\phi)^e}{\partial \{\phi\}^e} = [S]^e \{\phi\}^e + \{F\}^e, \tag{9}$$

where the elements of the matrix $[S]^e$ are given by

$$S^e_{nm} = \int_{R^e} \kappa_r r \frac{\partial N^e_n}{\partial r} \frac{\partial N^e_m}{\partial r} \, drdz$$

$$\int_{R^e} \kappa_z r \frac{\partial N^e_n}{\partial z} \frac{\partial N^e_m}{\partial z} \, drdz \quad ; \quad n,m = 1,\cdots,4,$$

and the elements of the vector $\{F\}^e$ are given by

$$F^e_n = \int_{C^e} qrN^e_n \, ds - \int_{R^e} \rho r N^e_n \, drdz \quad ; \quad n = 1,\cdots,4. \tag{11}$$

Equations giving the approximate set of potentials can now be obtained from equations (7) and (8) together with (9):

$$\frac{\partial I(\phi)}{\partial \phi_n} = \sum_e \frac{\partial I(\phi)^e}{\partial \phi_n} = 0 \tag{12}$$

$$\Rightarrow [S] \{\phi\} + \{F\} = 0, \tag{13}$$

$$S_{nm} = \sum_e S^e_{nm},$$

$$F_n = \sum_e F^e_n. \tag{14}$$

Note that the sums in (12) and (14) need to be taken only over those elements which share the node n, since

$$\frac{\partial I(\phi)^e}{\partial \phi_n} \equiv 0$$

if $I(\phi)^e$ does not contain ϕ_n (and hence node n).

We have yet to construct the matrix $[N]^e$. To do this, we need to find a function of the coordinates, r and z, which suitably describes the variation of ϕ over an element, and ensures convergence of the approximate minimization process given above. As was shown earlier, the function must also be of class C^1 on R^e and C^e to be admissible. This restriction can be shown to be sufficient to ensure convergence. provided the function can take on a constant value in an infinitesimal element [1].

Considering the above restrictions an appropriate function is the bilinear form

$$\phi = \alpha_1 + \alpha_2\xi + \alpha_3\eta + \alpha_4\xi\eta, \tag{15}$$

where ξ and η are local skewed coordinates defined as shown:

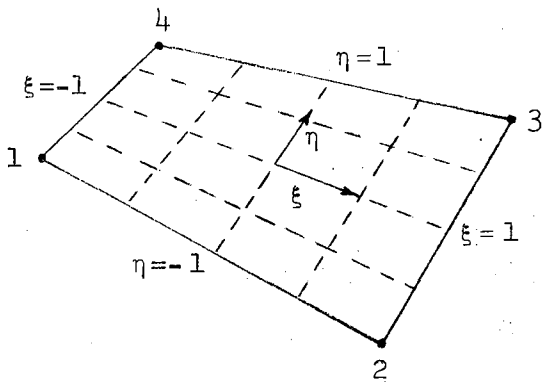

The values of ϕ at the four nodes of an element will then uniquely determine the four coefficients in (15) for that element, and hence

the components of $[N]^e$. Solving for the α's in terms of the nodal values of ϕ, we have the following expressions for $[N]^e$:

$$\begin{aligned} N_1^e &= \tfrac{1}{4}(1-\xi)(1-\eta), \\ N_2^e &= \tfrac{1}{4}(1+\xi)(1-\eta), \\ N_3^e &= \tfrac{1}{4}(1+\xi)(1+\eta), \\ N_4^e &= \tfrac{1}{4}(1-\xi)(1+\eta), \end{aligned} \tag{16}$$

where the local coordinated ξ and η are related to the global coordinates r and z by the formulas

$$\begin{aligned} z^e &= N_1^e z_1^e + N_2^e z_2^e + N_3^e z_3^e + N_4^e z_4^e, \\ r^e &= N_1^e r_1^e + N_2^e r_2^e + N_3^e r_3^e + N_4^e r_4^e. \end{aligned} \tag{17}$$

Equations (10) and (11) may now be used to obtain the elements of the matrix $[S]^e$ and the vector $\{F\}^e$, respectively, from (16) and (17):

$$S_{nm}^e = \kappa_r I_1(R^e) + \kappa_z I_2(R^e) \; ; \; n,m = 1,\cdots,4, \tag{18}$$

$$F_n^e = \rho I_3(R^e) + \sum_{j=1}^{4} q_j I_j(C^e) \; ; \; n = 1,\cdots,4, \tag{19}$$

where it has been assumed that the tensor $\underset{\sim}{\kappa}$ and the function $\rho(r,z)$ are constant over a given element, and that the function $q(s)$ is constant over a given boundary section between nodes. The quantities in (18) and (19) denoted by I_i (D) are easily evaluated by the application of Gaussian quadrature to the expressions listed below:

$$I_1(R^e) = \int_{-1}^{+1}\int_{-1}^{+1} \frac{r^e}{|J|^e}\left(\frac{\partial r^e}{\partial \eta}\frac{\partial N^e_n}{\partial \xi} - \frac{\partial r^e}{\partial \xi}\frac{\partial N^e_n}{\partial \eta}\right)\left(\frac{\partial r^e}{\partial \eta}\frac{\partial N^e_m}{\partial \xi} - \frac{\partial r^e}{\partial \xi}\frac{\partial N^e_m}{\partial \eta}\right) d\xi\, d\eta, \quad (20.1)$$

$$I_2(R^e) = \int_{-1}^{+1}\int_{-1}^{+1} \frac{r^e}{|J|^e}\left(\frac{\partial z^e}{\partial \xi}\frac{\partial N^e_n}{\partial \eta} - \frac{\partial z^e}{\partial \eta}\frac{\partial N^e_n}{\partial \xi}\right)\left(\frac{\partial z^e}{\partial \xi}\frac{\partial N^e_m}{\partial \eta} - \frac{\partial z^e}{\partial \eta}\frac{\partial N^e_m}{\partial \xi}\right) d\xi\, d\eta, \quad (20.2)$$

$$I_3(R^e) = -\int_{-1}^{+1}\int_{-1}^{+1} r^e N^e_n |J|^e d\xi\, d\eta, \quad (20.3)$$

$$I_1(C^e) = \int_{-1}^{+1} r^e N^e_n\, d\xi \quad ; \eta=-1, \quad (20.4)$$

$$I_2(C^e) = \int_{-1}^{+1} r^e N^e_n\, d\eta \quad ; \quad \xi=1, \quad (20.5)$$

$$I_3(C^e) = \int_{-1}^{+1} r^e N^e_n\, d\xi \quad ; \quad \eta=1, \quad (20.6)$$

$$I_4(C^e) = \int_{-1}^{+1} r^e N^e_n\, d\eta \quad ; \quad \xi=-1, \quad (20.7)$$

where $|J|^e$ is the Jacobian determinant

$$|J|^e = \left| \frac{\partial z^e}{\partial \xi}\frac{\partial r^e}{\partial \eta} - \frac{\partial z^e}{\partial \eta}\frac{\partial r^e}{\partial \xi} \right|. \quad (21)$$

The total matrix [S] and the total vector {F} are now obtained through the use of (14).

Modification of the Algorithm for 2-D Cartesian Systems

The mathematical model we have just given for cylindrically symmetric systems can, with only minor modification, be applied to two-dimensional Cartesian systems.

In Cartesian coordinates, equations (1) and (3) are, respectively,

$$\frac{\partial}{\partial x}\left(\kappa_x \frac{\partial \phi}{\partial x}\right) + \frac{\partial}{\partial y}\left(\kappa_y \frac{\partial \phi}{\partial y}\right) + \rho(x,y) = 0 \tag{22}$$

and

$$I(\phi) = \int_R \tfrac{1}{2}\left[\kappa_x\left(\frac{\partial \phi}{\partial x}\right)^2 + \kappa_y \left(\frac{\partial \phi}{\partial y}\right)^2 - 2\rho\phi\right] dxdy + \int_C q\,\phi\, ds. \tag{23}$$

Carrying the transformation through, we find the following expressions for the coupling matrix [S] and the boundary vector {F}:

$$S^e_{nm} = \int_{R^e} \kappa_x \frac{\partial N^e_m}{\partial x} \frac{\partial N^e_n}{\partial x}\, dxdy + \int_{R^e} \kappa_y \frac{\partial N^e_m}{\partial y} \frac{\partial N^e_n}{\partial y}\, dxdy \; ; \; n,m = 1,\cdots,4, \tag{24}$$

$$F^e_m = \int_{C^e} q\, N^e_n\, ds - \int_{R^e} \rho\, N^e_n\, dxdy \; ; \; n = 1,\cdots,4. \tag{25}$$

Since we have used the same type of element in both cases, all the statements made regarding regions and boundaries in the cylindrical development are valid here. In addition, the expressions given for the matrix $[N]^e$ in the cylindrical case are identical to those for the Cartesian case.

It is now apparent that all of the difference between the two systems is contained in the quantities

$$I_i\,(R^e) \quad ; \quad i = 1,2,3$$

and

$$I_i\,(C^e) \quad ; \quad i = 1,2,3,4.$$

Making the transformation $z \to x$ and $r \to y$ in (17), we find for the Cartesian case

$$I_1(R^e) = \int_{-1}^{+1}\int_{-1}^{+1} \frac{1}{|J|^e}\left(\frac{\partial y}{\partial \eta}^e \frac{\partial N}{\partial \xi}^e_n - \frac{\partial y}{\partial \xi}^e \frac{\partial N}{\partial \eta}^e_n\right)\left(\frac{\partial y}{\partial \eta}^e \frac{\partial N}{\partial \xi}^e_m - \frac{\partial y}{\partial \xi}^e \frac{\partial N}{\partial \eta}^e_m\right) d\xi\, d\eta, \qquad (26.1)$$

$$I_2(R^e) = \int_{-1}^{+1}\int_{-1}^{+1} \frac{1}{|J|^e}\left(\frac{\partial x}{\partial \xi}^e \frac{\partial N}{\partial \eta}^e_n - \frac{\partial x}{\partial \eta}^e \frac{\partial N}{\partial \xi}^e_n\right)\left(\frac{\partial x}{\partial \xi}^e \frac{\partial N}{\partial \eta}^e_m - \frac{\partial x}{\partial \eta}^e \frac{\partial N}{\partial \xi}^e_m\right) d\xi\, d\eta, \qquad (26.2)$$

$$I_3(R^e) = -\int_{-1}^{+1}\int_{-1}^{+1} N_n^e\, |J|^e\, d\xi\, d\eta, \qquad (26.3)$$

$$I_1(C^e) = \int_{-1}^{+1} N_n^e\, d\xi \quad ; \quad \eta = -1, \qquad (26.4)$$

$$I_2(C^e) = \int_{-1}^{+1} N_n^e\, d\eta \quad ; \quad \xi = 1, \qquad (26.5)$$

$$I_3(C^e) = \int_{-1}^{+1} N_n^e\, d\xi \quad ; \quad \eta = 1, \qquad (26.6)$$

$$I_4(C^e) = \int_{-1}^{+1} N_n^e\, d\eta \quad ; \quad \xi = -1, \qquad (26.7)$$

where

$$|J|^e = \left| \frac{\partial x}{\partial \xi}^e \frac{\partial y}{\partial \eta}^e - \frac{\partial x}{\partial \eta}^e \frac{\partial y}{\partial \xi}^e \right|. \qquad (27)$$

SOLUTION OF THE DIFFERENCE EQUATIONS

From (10) it is obvious that the matrix [S] is symmetric. Since a given node is coupled only with the nodes of the elements which share it, [S] is block tridiagonal. In addition, if we assume that

$$\kappa_r > 0 \; ; \; \kappa_z > 0 \tag{28}$$

[so that (1) is elliptic], it can be shown that [S] is positive definite. We may therefore apply the method of "normalized successive block overrelaxation" [3] to the solution of the system (13).

Partitioning [S] by rows into block tridiagonal form yields:

$$[S] = \begin{bmatrix} B_1 & C_2 & & & 0 \\ C_2 & B_2 & C_3 & & \\ & \ddots & \ddots & \ddots & \\ & & \ddots & \ddots & C_L \\ 0 & & & C_L & B_L \end{bmatrix}, \tag{29}$$

where the submatrices B_i and C_i are of order n_i, n_i being the number of mesh points on the ith row, and are all tridiagonal. Also, since [S] is symmetric and positive definite, it follows that all of the submatrices B_i , $i = 1, \cdots, L$ are symmetric and positive definite:

$$B_i = \begin{bmatrix} b_1 & c_1 & & & 0 \\ c_1 & b_2 & c_2 & & \\ & \ddots & \ddots & \ddots & \\ & & \ddots & \ddots & c_{n_i-1} \\ 0 & & & c_{n_i-1} & b_{n_i} \end{bmatrix}. \tag{30}$$

Since B_i is a real symmetric and positive definite tridiagonal matrix, it has the unique factorization

$$B_i = D_i T_i' T_i D_i \; ; \quad i = 1,\ldots L, \tag{31}$$

where

$$D_i = \begin{bmatrix} d_1 & & & 0 \\ & d_2 & & \\ & & \ddots & \\ 0 & & & d_{n_i} \end{bmatrix} \; ; \; d_1 = b_1^{\frac{1}{2}} \; ; \; d_j = \left[b_j - (c_{j-1}/d_{j-1})^2\right]^{\frac{1}{2}},$$

$$j = 2,\ldots,n_i,$$

and

$$T_i = \begin{bmatrix} 1 & e_1 & & & 0 \\ & 1 & e_2 & & \\ & & \ddots & \ddots & \\ & & & 1 & e_{n_i-1} \\ 0 & & & & 1 \end{bmatrix} \; ; \; e_j = c_j/(d_j d_{j+1}),$$

$$j = 1,\ldots,n_i-1.$$

With the vector of ϕ values and the vector of F values for the ith row denoted by Φ_i and G_i respectively, and with

$$X_i \equiv D_i \Phi_i \; , \; M_i \equiv -D_i^{-1} G_i \; ; \; i = 1,\ldots,L, \tag{33.1}$$

$$P_i \equiv -D_{i-1}^{-1} C_i D_i^{-1} \quad ; \quad i = 2,\cdots,L, \tag{33.2}$$

normalized successive block overrelaxation is defined by

$$(T_i' \; T_i) \; X_i^{*(m+1)} \equiv P_i X_{i-1}^{(m+1)} + P_{i+1} X_{i+1}^{(m)} + M_i, \tag{34.1}$$

$$X_i^{(m+1)} = \omega \, (X_i^{*(m+1)} - X_i^{(m)}) + X_i^{(m)}, \tag{34.2}$$

where m is the iteration number and ω is the overrelaxation factor.

The system of equations defined by (34.1) can be solved directly by the following algorithm:

$$h_i = g_1 \quad , \quad h_{j+1} = g_{j+1} - e_j h_j \quad ; \quad j = 1,\cdots,n_i-1, \tag{35.1}$$

$$x_{n_i} = h_{n_i} \quad , \quad x_j = h_j - e_j x_{j+1} \quad ; \quad j = 1,\cdots,n_i-1, \tag{35.2}$$

where we have denoted the jth component of the right-hand side of (34.1) by g_j. After the iteration given by (34.2) has converged, Φ_i can be obtained from the solution X_i by application of the relation

$$\Phi_i \equiv D_i^{-1} \; X_i. \tag{36}$$

Note that the entire process defined by (34.1) and (34.2) takes at most nine multiplications and ten additions per component per iteration, which is the same number as the point overrelaxation method requires. If the number of iterations is large, the time required to set up the matrices D_i , T_i , M_i, and P_i , and to obtain Φ_i from X_i, will be small compared with the total execution time. Since the rate of convergence of block iteration is theoretically faster than point iteration, its use in JASON will result in more efficient computation.

The optimum overrelaxation factor can be calculated from the largest eigenvalue of the iteration matrix just as in point overrelaxation [3]:

$$\omega_{opt} = 2/(1+\sqrt{1-\lambda}). \tag{37.1}$$

For $\omega < \omega_{opt}$, λ can be estimated from ω and the convergence rate, δ [4]:

$$\lambda = (\omega+\delta+1)/(\omega\sqrt{\delta}), \tag{37.2}$$

where δ is defined as

$$\delta = \|x^{m+1} - x^{m}\|/\|x^{m} - x^{m-1}\|, \tag{37.3}$$

m being the iteration number. We may therefore update our estimate for ω_{opt} at any stage of the iteration.

COMMENTS REGARDING THE PROGRAM

The use of quadrilaterals in the derivation of the JASON algorithm enables us to approximate any arbitrary boundary curve by a union of element sides. In this manner, boundary curves will always lie along mesh lines. As finer mesh spacing will be required in some regions to fit boundaries than in others, a nonuniform mesh is required. Construction of such a mesh by hand can be a formidable task, particularly since, for reasons of stability and accuracy, mesh variations should be smooth. To alleviate such problems, JASON has been provided with a mesh generator.

The method of generation used is that of "Equipotential Zoning" [5]. In this method, the mesh lines are regarded as two intersecting sets of equipotentials Φ and Ψ, which satisfy Laplace's equation in the interior of the region and take on successive integral values along the boundary. Performing a hodograph transformation on the equations $\nabla^2\Phi = 0$ and $\nabla^2\Psi = 0$ produces two new equations which will yield the coordinates of the mesh points (intersections of Φ lines and Ψ lines) directly. These equations are replaced by their representation in finite differences and solved by successive point overrelaxation.

Since it may be difficult to estimate the execution time required for some problems, a restart procedure is provided. The mesh coordinates and the iteration matrices are stored on magnetic tape as soon as they are generated. If it appears that the time limit will be exceeded before the iteration has converged, the current values for the elements of the solution vector are dumped on the tape. Execution may then be initiated

at this point, in a succeeding run, by reading in the dump tape. The control cards, input at the start of the program, will ensure that the tape is read and that execution resumes at the proper point.

During the iteration phase, the parameters ϵ, δ, and ω, are printed every few cycles to monitor the convergence. Two of these, ω and δ, have been defined previously in (37.1) and (37.3), respectively. The parameter ϵ, which is just the Euclidean norm of the relative error, is defined by

$$\epsilon = \|x^n - x^{n-1}\|/\|x^n\|, \tag{38}$$

where n denotes the iteration number and x denotes an element of the solution vector X, defined by (33.1). For convergence, it is normally required that ϵ be less than 10^{-7}. Once this criterion is satisfied, the iteration is terminated and the solution vector is calculated from (36).

In most cases, it is not the potential that is of interest, but the negative of its gradient. A set of subroutines for calculating the negative gradient of ϕ is therefore written into JASON. The edit routine fits a harmonic polynomial, in the least-squared sense, to a specified set of mesh points surrounding the point of evaluation. The derivatives of the polynomial are then taken as approximations to the derivatives of the potential. To produce better averaging of error, the centroids of the mesh elements, rather than the nodes, are taken as the points of evaluation. If the problem has $\partial\phi/\partial n=0$ on the lower universe boundary, as in the case of cylindrical symmetry, an edit is also taken at the centers of the element sides composing this boundary.

INPUT TO JASON

The several tasks performed by JASON are under the control of five "execution" control cards. These cards and their functions, briefly stated, are as follows:

(1) GENERATE ** based on the input data, JASON will generate a nonuniform quadrilateral mesh and calculate all values needed for solution;

(2) SOLVE ** solve for the potential (ϕ) in the above mesh (no input data required);

(3) EDIT ** calculate the negative gradient of the potential at quadrilateral centroids (no input data required);

(4) MPLOT ** plot the generated mesh showing all regions and boundaries (no input data required);

(5) VPLOT ** plot N equipotential lines, where N is an input quantity (integer) less than 101.

Any or all of the five options may be used in a run; however, ordering of events must be observed, i.e., GENERATE precedes all, SOLVE precedes EDIT, MPLOT, and VPLOT, etc. In addition, if either GENERATE or SOLVE is missing, the program assumes that the dump tape (TAPE35) is to be read in. Each option is punched on a single card starting in column one. A blank card must follow the last control card to signal the end of control information.

The complete problem description, including mesh size, material regions, and boundaries (Neumann, Dirichlet), is input in the GENERATE phase. If the problem has cylindrical symmetry (LIN = 0), the lower universe boundary is automatically set to $\partial\phi/\partial n = 0$ by JASON. The other

universe boundaries are specified by the code as Dirichlet with $\phi = 0$, but may be set otherwise if proper input cards are entered (see D and E below). If the problem is given in two-dimensional Cartesian coordinates (LIN=1), JASON sets all the universe boundaries to Dirichlet with $\phi = 0$. As in the cylindrical case, these specifications may be changed by appropriate input. The following list describes the GENERATE phase input in detail. The order of the list is the same as that which must appear in the data deck. All input is format-free, the only requirement being that entries be separated by one or more blanks.

A. Name Card ** This card may contain any information punched in columns 1-80. It will be used as an identifier on the printed output and the plots.

B. Mesh Info. ** The next card must define the maximum K and L coordinates (KMAX,LMAX), the number of material regions (NR), including the universe, and the sentinel LIN, as described above:

KMAX LMAX NR LIN

All values are type integer. LMAX*KMAX must not exceed the dimension of the program arrays.

C. Material Regions ** NR sets of region cards are required, one for each closed material region. The first card of each set must contain the number of points used to define the region, the material constants, KR and KZ, and the source density, RHO:

NP KR KZ RHO

NP is an integer, while KR, KZ, and RHO are floating-point. The first set of region cards must define the universe. The remaining NR-1 subregions will override the values of KR, KZ, and RHO set by

the universe. For each of the NP points, a card must be input to give the mesh coordinates (K,L) and the point coordinates (X,Y):

K L X Y ,

where K and L are integers, and X and Y are floating point. Since regions are defined along lines of constant K or constant L, for any two consecutive points it is required that $K_i = K_{i+1}$ or $L_i = L_{i+1}$, but not both. Also, since the regions are closed, $(K,L,X,Y)_1=(K,L,X,Y)_{NP}$, i.e., the first and last points must coincide.

D. Neumann Boundaries ** Neumann boundary conditions may be specified only on the edges of the previously defined material regions. Input consists of the mesh coordinates of the first point (K1,L1), the mesh coordinates of the last point (K2,L2), an integer designating the direction of the normal (IQ), and the value of the normal derivtive (Q):

K1 L1 K2 L2 IQ Q ,

where all the entries are integers except Q, which is floating-point. As before, K1 = K2 or L1 = L2, but not both. The normal directions are specified as follows:

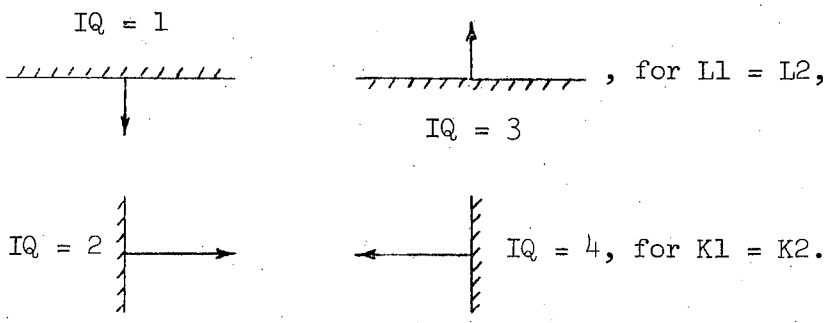

The normal direction must be taken as outward from the universe or or region of interest. If the boundary condition is to be imposed on a universe boundary or section thereof, it is restricted to contain at least three points, i.e., $|L1-L2|\geq 2$ or $|K1-K2|\geq 2$. For an interface between two regions, cards must be input for both regions, i.e., for each Neumann interface card with IQ = J, J = 1, 2, and Q = q_1, there is a second card which is identical except for having IQ = J+1 and Q = q_2. This results in an interface condition of the form

$$(\underset{\sim}{\kappa}_1 \underset{\sim}{\nabla} \phi)_{n+} - (\underset{\sim}{\kappa}_2 \underset{\sim}{\nabla} \phi)_{n-} + q_1 + q_2 = 0, \qquad (39)$$

where n denotes the normal direction outward from the region with material tensor $\underset{\sim}{\kappa}_1$, and n+ denotes evaluation of the function on the side of the interface containing material 1 (with n- conversely). Observe that when the region on one side of the interface has (KR,KZ)=0 (or undefined, as in the case of the universe boundary), equation (39) reduces to equation (4). In this case only one card is needed with the normal specified as outward from the region having (KR,KZ) $\neq$0. If $q_1 = -q_2$ or q = 0, no boundary cards need be input. The interface or Neumann condition will be automatically satisfied.

Following the Neumann boundary cards, there must be a card punched

0 S .

This card must be present even if no Neumann boundaries are specified.

E. Dirichlet Boundaries ** A set of cards is needed for each Dirichlet boundary. The first card will give the number of points (NP) used to describe the boundary, and the potential (ϕ) at each of the in-

clusive points. As in the material regions, NP cards must follow giving (K,L,X,Y) for each point. Again we have the restriction that for any two consecutive cards $K_i = K_{i+1}$ or $L_i = L_{i+1}$, but not both. The last card must be punched

0 0.

This card must be present, even if no Dirichlet boundaries are specified, as it terminates the reading of data input for the GENERATE phase.

In all cases the dump tape (TAPE35) is required for execution. In addition, JASON requires a TAPE1 for the GENERATE and MPLOT phases. This tape is used to store the region information input in the GENERATE phase. MPLOT then uses this information in producing the mesh plot.

POSSIBLE EXTENSIONS OF JASON

General Anisotropy

In deriving the system of equations (13) from (1), it was assumed that the tensor $\underset{\sim}{K}$ was diagonal in the global coordinate system. Obviously, this restricts us to consideration of problems in which the principal axes of all materials are parallel to the global coordinate axes. This restriction can be removed by assuming $\underset{\sim}{K}$ to be diagonal in some local coordinate system for each element in the mesh. The axes of this local coordinate system are then parallel to the principal axes of the material in that element. Equation (1) is now the governing differential equation in the local coordinate system for each element, and expression (19) may be evaluated for each element using local coordinates. These results are then transformed to the global system before assembly, as specified by (14), into the total [S] matrix and {F} vector. Therefore, if we know the transformation from local to global coordinates for each element, problems with general anisotropy may be considered.

Nonlinear Problems

If we allow the tensor $\underset{\sim}{K}$ to be a function of ϕ or its derivatives, equation (1) becomes nonlinear. If we use a restricted variation [4], however, this in no way effects our derivation of the system of equations (13). Only our method of solution needs to be changed. A method such as "Linearized Successive Overrelaxation" [4] could be applied to solve the nonlinear system (13). As $\underset{\sim}{K}$ will change in value as the iteration progresses, it is obvious from (18) that more storage will be required

than for linear problems.

Acknowledgements

We wish to thank Mr. J. S. Colonias for his interest and support throughout this work. We also wish to thank Dr. P. Concus, to whom we are indebted for checking the derivation of the equations invloved. In addition, we are indebted to Dr. F. Resmini for permission to use his electrostatic quadrupole as an example.

REFERENCES

[1] O. C. Zienkiewics, The Finite Element Method in Structural and Continuum Mechanics, (McGraw -Hill, Inc., London, 1967)

[2] O. Bolza, Lectures on the Calculus of Variation, (Dover Publications, Inc., 1961)

[3] E. H. Cuthill, and R. S. Varga, "A Method of Normalized Block Iteration", Journal of the Association for Computing Machinery, Vol. 6 (1959), pp. 236-244.

[4] A. Winslow, Numerical Solution of the Poisson Equation in a Non-Uniform Triangle Mesh, Lawrence Radiation Laboratory report UCRL-7784-T (Rev. 2), August, 1965.

[5] A. Winslow, Equipotential Zoning of Two-Dimensional Meshes, Lawrence Radiation Laboratory report UCRL- 7321, June, 1963.

APPENDIX A

Expressions for the Partial Derivatives in (20.1) - (21)

$$\frac{\partial r^e}{\partial \xi} = \tfrac{1}{4}[(1-\eta)(r_2^e - r_1^e) + (1+\eta)(r_3^e - r_4^e)] \tag{A1.1}$$

$$\frac{\partial r^e}{\partial \eta} = \tfrac{1}{4}[(1-\xi)(r_4^e - r_1^e) + (1+\xi)(r_3^e - r_2^e)] \tag{A1.2}$$

$$\frac{\partial z^e}{\partial \xi} = \tfrac{1}{4}[(1-\eta)(z_2^e - z_1^e) + (1+\eta)(z_3^e - z_4^e)] \tag{A2.1}$$

$$\frac{\partial z^e}{\partial \eta} = \tfrac{1}{4}[(1-\xi)(z_4^e - z_1^e) + (1+\xi)(z_3^e - z_2^e)] \tag{A2.2}$$

$$\frac{\partial N_1^e}{\partial \xi} = -\tfrac{1}{4}(1-\eta) \quad , \quad \frac{\partial N_1}{\partial \eta} = -\tfrac{1}{4}(1-\xi) \tag{A3}$$

$$\frac{\partial N_2^e}{\partial \xi} = \tfrac{1}{4}(1-\eta) \quad , \quad \frac{\partial N_2^e}{\partial \eta} = -\tfrac{1}{4}(1+\xi) \tag{A4}$$

$$\frac{\partial N_3^e}{\partial \xi} = \tfrac{1}{4}(1+\eta) \quad , \quad \frac{\partial N_3^e}{\partial \eta} = \tfrac{1}{4}(1+\xi) \tag{A5}$$

$$\frac{\partial N_4^e}{\partial \xi} = -\tfrac{1}{4}(1+\eta) \quad , \quad \frac{\partial N_4^e}{\partial \eta} = \tfrac{1}{4}(1-\xi) \tag{A6}$$

APPENDIX B

Harmonic polynomials for Cylindrical Edit

$$V(r,z) = a_o + a_1 z + a_2(z^2-r^2/2) + a_3(z^3-3r^2z/2) + a_4(z^4-3r^2z^2+3r^4/8). \quad (B.1)$$

Harmonic polynomials for Cartesian Edit

$$V(x,y) = a_o + a_1 x + a_2 y + a_3 xy + a_4(x^2-y^2) + a_5(x^3-3xy^2) + a_6(y^3-3x^2y). \quad (B.2)$$

$$V(x,y) = a_o + a_1 x + a_4(x^2-y^2) + a_5(x^3-3xy^2), \quad (B.3)$$

for the case of symmetry about the x-axis.

APPENDIX C

Sample Input to JASON

Figure 1 shows a problem in electrostatics which may be run on JASON. It is a contrived problem which serves only to exemplify the input setup. The problem, which has cylindrical symmetry, consists of a perfectly conducting paraboloid (A), a perfectly conducting disc (B), a small disc of charge (c), and a dielectric disc (D). The "universe" in which this construction is enclosed consists of two grounded, perfectly conducting discs 40 cm apart, and a perfectly insulating cylinder 30 cm in radius.

The first step is to decide on a mesh size and overlay the problem geometry. Figure 2 shows a logical diagram for the problem in mesh with KMAX = 41 and LMAX = 31. Observe that grid A has been represented by a straight line in mesh coordinates. Figure 3 shows grid A zoned to more nearly approximate the parabola. For the sample run, the zoning shown in Figure 2 was chosen as it will demonstrate the mesh distortions that can result from poor zoning.

There are 3 material regions to input, i.e., the universe, region C, and region D. The problem has cylindrical symmetry, thus our first two cards are:

1. SAMPLE CASE USING VARIOUS FEATURES OF JASON

2. 41 31 3 0 ;

and the universe region card is

10 1. 1. 0.

K_i L_i Z_i R_i } 10 cards

(see Appendix D for a listing of the 10 points). The 10 points include the four corners, and the 5 points which touch the lower boundary at grid A, grid B, region C, and region D. Since regions C and D are rectangular and straight (in r-z coordinates), only 5 points are needed to describe each of them:

5 1. 1. 100.

K_i L_i Z_i R_i } 5 cards,

for region 2, and

5 7. 7. 0.

K_i L_i Z_i R_i } 5 cards,

for region 3 (see Appendix D for a listing of K, L, Z, R for the above).

The upper boundary is reflective, so a Neumann condition must be imposed:

1 31 41 31 3 0.

A card punched

0 S

must follow this to terminate reading of these boundaries.

The two grids, A and B, are Dirichlet boundaries. Grid B is the simplest to describe since it is straight, i.e., z is constant. The input cards required are:

2 1000.

27 1 25. 0.

27 16 25. 15.

Grid A is neither constant in z nor constant in r, so all 17 points must be input:

17 -1000.

K_i L_i Z_i R_i } 17 cards

(see Appendix D for a listing of the points). Finally, a card punched

0 0.

is required to terminate the GENERATE data set.

Figure 4 shows the plot of the generated mesh (MPLOT option). This mesh could have been made more uniform by using the logical diagram for grid A shown in figure 3 rather than that of figure 2. Figure 5 shows an equipotential plot for this sample case. The last card in the data deck contains

25

to indicate to the VPLOT option that 25 contour lines are to be plotted.

PROGRAMMER _ APPENDIX D

PROBLEM _____ EXT. _____

FORTRAN

C ← FOR COMMENT | STATEMENT NUMBER | CONT | FORTRAN STATEMENT

```
      INPUT FOR JASON
      SAMPLE CASE
GENERATE
SOLVE
EDIT
MPLOT
VPLOT
      Blank card (required)
SAMPLE CASE USING VARIOUS FEATURES OF JASON
$ ANY TEXT ENCLOSED IN DOLLAR SIGNS WILL BE TREATED AS A COMMENT. $
$ NO COMMENTS ARE PERMITTED BEFORE THE NAME CARD. $

   41    31    3    0    $ KMAX   LMAX   NR   LIN $

   10    1.    1.    0.   $ BEGIN REGION 1 $
    1    1     0.    0.
   11    1    10.    0.
   24    1    23.    0.
   25    1    23.5   0.
   27    1    25.    0.
   31    1    30.    0.
   41    1    40.    0.
   41   31    40.   30.
    1   31     0.   30.
    1    1     0.    0.    $ END REGION 1 $

    5    1.    1.   100.   $ BEGIN REGION 2 $
   24    1    23.    0.
   25    1    23.5   0.
```

PROGRAMMER _____

PROBLEM _____ EXT. _____

FORTRAN

C ← FOR COMMENT | STATEMENT NUMBER | CONT | FORTRAN STATEMENT

```
      25     2      23.5    1.
      24     2      23.     1.
      24     1      23.     0.     $ END REGION 2 $

       5     7.     7.      0.     $ BEGIN REGION 3 $
      27     1      25.     0.
      27    16      25.    15.
      31    16      30.    15.
      31     1      30.     0.
      27     1      25.     0.     $ END REGION 3 $

       1    31     41 31     3     0. $ NEUMANN BOUNDARY $

       0     S     $ THIS CARD REQUIRED $

       2     1000. $ BEGIN DIRICHLET BOUNDARY 1 (GRID B) $
      27     1      25.     0.
      27    16      25.    15. $ END D.B. 1 $

      17    -1000. $ BEGIN DIRICHLET BOUNDARY 2 (GRID A) $
      11     1      10.     0.
      11     2      10.03125     1.
      11     3      10.125       2.
      11     4      10.28125     3.
      11     5      10.5         4.
      11     6      10.78125     5.
      11     7      11.125       6.
```

PROGRAMMER _____

PROBLEM _____ EXT. _____

FORTRAN

C ← FOR COMMENT | STATEMENT NUMBER | CONT | FORTRAN STATEMENT

```
      11      8      11.53125      7.
      11      9      12.           8.
      11     10      12.53125      9.
      11     11      13.125       10.
      11     12      13.78125     11.
      11     13      14.5         12.
      11     14      15.28125     13.
      11     15      16.125       14.
      11     16      17.03125     15.
      11     17      18.          16. $ END D.B. 2 $

      0       0.     $ THIS CARD REQUIRED $ $ END GENERATE DATA $

      25      $ PL$T N=25 EQUIP$TENTIAL LINES $

$     END   DATA    $
```

PROGRAMMER _ APPENDIX E

PROBLEM _____ EXT. _____

FORTRAN

C ← FOR COMMENT | STATEMENT NUMBER | CONT | FORTRAN STATEMENT

```
      SAMPLE DECK SETUP FOR
      BKY CHIPPEWA OPERATING SYSTEM
JASON,S,200,110000.424201,SACKETT
REQUEST TAPE35. JASON DUMP TAPE
REWIND(TAPE35)
REQUEST TAPE1. JASON MPLOT TAPE
REWIND(TAPE1)
REQUEST TAPE99. CALCOMP PLOT TAPE
REWIND(TAPE99)
RUN(G)
COPYBF(NULL,TAPE35)
UNLOAD(TAPE35)
UNLOAD(TAPE1)
7 8 9          (multiple punch in column 1)
               JASON Program Deck
7 8 9          (multiple punch in column 1)
               JASON Data Deck
6 7 8 9        (multiple punch in column 1)
```

APPENDIX F.

OUTPUT FROM SAMPLE CASE

SAMPLE CASE USING VARIOUS FEATURE OF JASON

CYLINDRICAL SYMMETRY

KMAX= 41
LMAX= 31

3 MATERIAL REGIONS -----

REGION 1 10 POINTS KR/KY= 1.00000E+00 KZ/KX= 1.00000E+00 RHO= 0.

K	L	Z/X	R/Y
1	1	0.	0.
11	1	10.000000	0.
24	1	23.000000	0.
25	1	23.500000	0.
27	1	25.000000	0.
31	1	30.000000	0.
41	1	40.000000	0.
41	31	40.000000	30.000000
1	31	0.	30.000000
1	1	0.	0.

REGION 2 5 POINTS KR/KY= 1.00000E+00 KZ/KX= 1.00000E+00 RHO= 1.00000E+02

K	L	Z/X	R/Y
24	1	23.000000	0.
25	1	23.500000	0.
25	2	23.500000	1.000000
24	2	23.000000	1.000000
24	1	23.000000	0.

REGION 3 5 POINTS KR/KY= 7.00000E+00 KZ/KX= 7.00000E+00 RHO= 0.

K	L	Z/X	R/Y
27	1	25.000000	0.
27	16	25.000000	15.000000
31	16	30.000000	15.000000
31	1	30.000000	0.
27	1	25.000000	0.

NEUMANN BOUNDARIES -----

	K1	L1	K2	L2	SIDE	VALUE
1	1	31	41	31	3	0.

DIRICHLET BOUNDARIES -----

2 POINTS WITH POTENTIAL 1000.0000

K	L	Z/X	R/Y
27	1	25.000000	0.
27	16	25.000000	15.000000

17 POINTS WITH POTENTIAL -1000.0000

K	L	Z/X	R/Y
11	1	10.000000	0.
11	2	10.031250	1.000000
11	3	10.125000	2.000000
11	4	10.281250	3.000000
11	5	10.500000	4.000000
11	6	10.781250	5.000000
11	7	11.125000	6.000000
11	8	11.531250	7.000000
11	9	12.000000	8.000000
11	10	12.531250	9.000000
11	11	13.125000	10.000000
11	12	13.781250	11.000000
11	13	14.500000	12.000000
11	14	15.281250	13.000000
11	15	16.125000	14.000000
11	16	17.031250	15.000000
11	17	18.000000	16.000000

CYCLE	CONX	CONY	RHOX	RHOY
2	.008750190	.000000000	1.600000	1.600000
3	.009442887	.000000000	1.600000	1.600000
4	.004681089	.000000000	1.600000	1.600000
5	.004287016	.000000000	1.600000	1.600000
53	.000000533	.000000000	1.754197	1.933059
54	.000000420	.000000000	1.754197	1.933059
55	.000000330	.000000000	1.752118	1.933059
56	.000000256	.000000000	1.752118	1.933059

MESH CONVERGED IN 8.860 SECONDS *** *** ***

TOTAL GENERATION TIME (INPUT, MESH, COUPLINGS) IS 22.630 SECONDS ***

SAMPLE CASE USING VARIOUS FEATURE OF JASON

CYCLE	RESIDUAL/LENGTH	ETA	OMEGA
5	9.573082E-02	7.339291E-01	1.543825
10	2.545261E-02	7.927697E-01	1.598281
15	8.651603E-03	8.036985E-01	1.639139
20	3.486743E-03	8.555828E-01	1.690728
25	1.996238E-03	8.756749E-01	1.733917
30	1.214129E-03	8.881173E-01	1.767805
35	7.821747E-04	8.980839E-01	1.794622
40	4.944792E-04	8.889433E-01	1.808608
45	2.703567E-04	8.657303E-01	1.811752
50	1.218492E-04	8.369745E-01	1.809383
55	4.474595E-05	8.078318E-01	1.805638
60	1.349362E-05	7.810448E-01	1.803245
65	3.349595E-06	7.614643E-01	1.803507
70	6.733424E-07	7.818117E-01	1.800798
75	1.508963E-07	9.573081E-01	1.853679
80	1.188036E-07	9.015228E-01	1.856178
85	5.979263E-08	8.488398E-01	1.852582
90	1.847556E-08	7.758597E-01	1.868906
97	1.009478E-09	9.264783E-01	1.426285

PROBLEM CONVERGED IN 8.522 SECONDS *** *** ***

L	K	Z	R	V
1	1	0.	0.	0.
1	2	1.000	0.	-8.16402E+01
1	3	2.000	0.	-1.64220E+02
1	4	3.000	0.	-2.48710E+02
1	5	4.000	0.	-3.36142E+02
1	6	5.000	0.	-4.27646E+02
1	7	6.000	0.	-5.24506E+02
1	8	7.000	0.	-6.28218E+02
1	9	8.000	0.	-7.40583E+02
1	10	9.000	0.	-8.63888E+02
1	11	10.000	0.	-1.00000E+03
1	12	11.000	0.	-9.24716E+02
1	13	12.000	0.	-8.41337E+02
1	14	13.000	0.	-7.48686E+02
1	15	14.000	0.	-6.46558E+02
1	16	15.000	0.	-5.34871E+02
1	17	16.000	0.	-4.13712E+02
1	18	17.000	0.	-2.83332E+02
1	19	18.000	0.	-1.44152E+02
1	20	19.000	0.	3.26299E+00
1	21	20.000	0.	1.58237E+02
1	22	21.000	0.	3.20158E+02
1	23	22.000	0.	4.88719E+02
1	24	23.000	0.	6.71284E+02
1	25	23.500	0.	7.57147E+02
1	26	24.250	0.	8.74703E+02
1	27	25.000	0.	1.00000E+03
1	28	26.250	0.	9.78741E+02
1	29	27.500	0.	9.57689E+02
1	30	28.750	0.	9.38384E+02
1	31	30.000	0.	8.89922E+02
1	32	31.000	0.	8.19497E+02
1	33	32.000	0.	7.24758E+02
1	34	33.000	0.	6.30899E+02
1	35	34.000	0.	5.37719E+02
1	36	35.000	0.	4.45702E+02
1	37	36.000	0.	3.54865E+02
1	38	37.000	0.	2.65104E+02
1	39	38.000	0.	1.76218E+02
1	40	39.000	0.	8.79500E+01
1	41	40.000	0.	0.

L	K	Z	R	V
2	1	0.	1.000	0.
2	2	1.017	1.000	-8.26750E+01
2	3	2.033	1.000	-1.66313E+02
2	4	3.049	1.000	-2.51900E+02
2	5	4.064	1.000	-3.40471E+02
2	6	5.078	1.000	-4.33132E+02
2	7	6.089	1.000	-5.31075E+02
2	8	7.095	1.000	-6.35579E+02
2	9	8.093	1.000	-7.47958E+02
2	10	9.077	1.000	-8.69302E+02
2	11	10.031	1.000	-1.00000E+03
2	12	11.099	1.000	-9.19926E+02
2	13	12.139	1.000	-8.32167E+02
2	14	13.161	1.000	-7.36046E+02
2	15	14.171	1.000	-6.31307E+02
2	16	15.170	1.000	-5.17984E+02
2	17	16.161	1.000	-3.96311E+02
2	18	17.144	1.000	-2.66692E+02
2	19	18.119	1.000	-1.29678E+02
2	20	19.087	1.000	1.40655E+01
2	21	20.049	1.000	1.63870E+02
2	22	21.008	1.000	3.19422E+02
2	23	21.975	1.000	4.82282E+02
2	24	23.000	1.000	6.61630E+02
2	25	23.500	1.000	7.47536E+02
2	26	24.249	1.000	8.72729E+02
2	27	25.000	1.000	1.00000E+03
2	28	26.250	1.000	9.78653E+02
2	29	27.500	1.000	9.57673E+02
2	30	28.750	1.000	9.37137E+02
2	31	30.000	1.000	9.14764E+02
2	32	31.000	1.000	8.18890E+02
2	33	32.000	1.000	7.24825E+02
2	34	33.000	1.000	6.30540E+02
2	35	34.000	1.000	5.37303E+02
2	36	35.000	1.000	4.45282E+02
2	37	36.000	1.000	3.54487E+02
2	38	37.000	1.000	2.64796E+02
2	39	38.000	1.000	1.76002E+02
2	40	39.000	1.000	8.78384E+01
2	41	40.000	1.000	0.

L	K	Z	R	V
3	1	0.	2.000	0.
3	2	1.034	2.000	-8.33377E+01
3	3	2.067	2.000	-1.67654E+02
3	4	3.100	2.000	-2.53943E+02
3	5	4.131	2.000	-3.43237E+02
3	6	5.160	2.000	-4.36605E+02
3	7	6.184	2.000	-5.35155E+02
3	8	7.199	2.000	-6.39985E+02
3	9	8.201	2.000	-7.52076E+02
3	10	9.181	2.000	-8.72086E+02
3	11	10.125	2.000	-1.00000E+03
3	12	11.235	2.000	-9.16136E+02
.	.	.	.	.
.	.	.	.	.
.	.	.	.	.
21	1	0.	20.000	0.
21	2	1.189	20.000	-3.54425E+01
21	3	2.382	20.000	-7.07971E+01
21	4	3.581	20.000	-1.05962E+02
21	5	4.789	20.000	-1.40807E+02
21	6	6.011	20.000	-1.75147E+02
21	7	7.250	20.000	-2.08718E+02
21	8	8.510	20.000	-2.41134E+02
21	9	9.792	20.000	-2.71875E+02
21	10	11.100	20.000	-3.00234E+02
21	11	12.439	20.000	-3.25137E+02
21	12	13.752	20.000	-3.43371E+02
21	13	14.967	20.000	-3.50757E+02
21	14	16.051	20.000	-3.44042E+02
21	15	17.017	20.000	-3.22263E+02
21	16	17.892	20.000	-2.86887E+02
21	17	18.705	20.000	-2.41451E+02
21	18	19.479	20.000	-1.89370E+02
21	19	20.231	20.000	-1.33383E+02
21	20	20.973	20.000	-7.55689E+01
21	21	21.714	20.000	-1.75514E+01
21	22	22.462	20.000	3.92608E+01
21	23	23.222	20.000	9.34901E+01
21	24	23.999	20.000	1.43704E+02
21	25	24.798	20.000	1.88401E+02
21	26	25.624	20.000	2.26146E+02
21	27	26.480	20.000	2.55666E+02
21	28	27.367	20.000	2.76059E+02
21	29	28.282	20.000	2.86908E+02
21	30	29.219	20.000	2.88418E+02
21	31	30.174	20.000	2.81369E+02
21	32	31.139	20.000	2.66988E+02
21	33	32.113	20.000	2.46730E+02
21	34	33.092	20.000	2.22042E+02
21	35	34.074	20.000	1.94184E+02
21	36	35.058	20.000	1.64147E+02
21	37	36.045	20.000	1.32645E+02
21	38	37.033	20.000	1.00176E+02
21	39	38.021	20.000	6.70866E+01
21	40	39.011	20.000	3.36292E+01
21	41	40.000	20.000	0.

L	K	Z	R	V
4	1	0.	3.000	0.
4	2	1.052	3.000	-8.35932E+01
4	3	2.104	3.000	-1.68176E+02
4	4	3.154	3.000	-2.54751E+02
4	5	4.204	3.000	-3.44346E+02
4	6	5.249	3.000	-4.38009E+02
4	7	6.289	3.000	-5.36792E+02
4	8	7.320	3.000	-6.41697E+02
4	9	8.334	3.000	-7.53572E+02
4	10	9.325	3.000	-8.72966E+02
4	11	10.281	3.000	-1.00000E+03
4	12	11.416	3.000	-9.13137E+02
.	.	.	.	.
.	.	.	.	.
.	.	.	.	.
22	1	0.	21.000	0.
22	2	1.172	21.000	-3.21186E+01
22	3	2.345	21.000	-6.40795E+01
22	4	3.524	21.000	-9.57101E+01
22	5	4.710	21.000	-1.26807E+02
22	6	5.906	21.000	-1.57113E+02
22	7	7.112	21.000	-1.86297E+02
22	8	8.332	21.000	-2.13919E+02
22	9	9.565	21.000	-2.39390E+02
22	10	10.808	21.000	-2.61901E+02
22	11	12.057	21.000	-2.80275E+02
22	12	13.285	21.000	-2.92619E+02
22	13	14.455	21.000	-2.96771E+02
22	14	15.544	21.000	-2.91025E+02
22	15	16.548	21.000	-2.74685E+02
22	16	17.479	21.000	-2.48298E+02
22	17	18.354	21.000	-2.13440E+02
22	18	19.188	21.000	-1.72265E+02
22	19	19.996	21.000	-1.26892E+02
22	20	20.789	21.000	-7.91841E+01
22	21	21.576	21.000	-3.07326E+01
22	22	22.365	21.000	1.70593E+01
22	23	23.162	21.000	6.28896E+01
22	24	23.970	21.000	1.05501E+02
22	25	24.796	21.000	1.43679E+02
22	26	25.642	21.000	1.76294E+02
22	27	26.511	21.000	2.02385E+02
22	28	27.403	21.000	2.21247E+02
22	29	28.317	21.000	2.32535E+02
22	30	29.250	21.000	2.36312E+02
22	31	30.199	21.000	2.33039E+02
22	32	31.159	21.000	2.23501E+02
22	33	32.127	21.000	2.08672E+02
22	34	33.102	21.000	1.89581E+02
22	35	34.081	21.000	1.67190E+02
22	36	35.064	21.000	1.42328E+02
22	37	36.049	21.000	1.15667E+02
22	38	37.035	21.000	8.77302E+01
22	39	38.023	21.000	5.89289E+01
22	40	39.011	21.000	2.95923E+01
22	41	40.000	21.000	0.

29	38	37.015	28.000	4.86721E+01	30	38	37.008	29.000	3.91175E+01
29	39	38.010	28.000	2.77154E+01	30	39	38.005	29.000	2.66752E+01
29	40	39.005	28.000	1.40383E+01	30	40	39.002	29.000	1.35172E+01
29	41	40.000	28.000	0.	30	41	40.000	29.000	0.

L	K	Z	R	V
31	1	0.	29.000	0.
31	2	1.018	29.000	-1.77879E+01
31	3	2.035	29.000	-3.53337E+01
31	4	3.053	29.000	-5.23936E+01
31	5	4.071	29.000	-6.87210E+01
31	6	5.088	29.000	-8.40651E+01
31	7	6.106	29.000	-9.81712E+01
31	8	7.124	29.000	-1.10781E+02
31	9	8.141	29.000	-1.21637E+02
31	10	9.159	29.000	-1.30483E+02
31	11	10.174	29.000	-1.37076E+02
31	12	11.189	29.000	-1.41193E+02
31	13	12.200	29.000	-1.42647E+02
31	14	13.210	29.000	-1.41298E+02
31	15	14.217	29.000	-1.37074E+02
31	16	15.220	29.000	-1.29983E+02
31	17	16.220	29.000	-1.20130E+02
31	18	17.216	29.000	-1.07718E+02
31	19	18.209	29.000	-9.30558E+01
31	20	19.199	29.000	-7.65442E+01
31	21	20.186	29.000	-5.86661E+01
31	22	21.171	29.000	-3.99637E+01
31	23	22.154	29.000	-2.10138E+01
31	24	23.138	29.000	-2.40088E+00
31	25	24.121	29.000	1.53098E+01
31	26	25.105	29.000	3.15972E+01
31	27	26.090	29.000	4.60058E+01
31	28	27.076	29.000	5.81624E+01
31	29	28.064	29.000	6.77870E+01
31	30	29.053	29.000	7.46986E+01
31	31	30.043	29.000	7.88141E+01
31	32	31.035	29.000	8.01435E+01
31	33	32.029	29.000	7.87801E+01
31	34	33.023	29.000	7.48887E+01
31	35	34.018	29.000	6.86924E+01
31	36	35.014	29.000	6.04598E+01
31	37	36.011	29.000	5.04929E+01
31	38	37.008	29.000	3.91175E+01
31	39	38.005	29.000	2.66752E+01
31	40	39.002	29.000	1.35172E+01
31	41	40.000	29.000	0.

SAMPLE CASE USING VARIOUS FEATURE OF JASON

HARMONIC POLYNOMIAL EDIT *** CYLINDRICAL SYMMETRY

DERIVATIVES ARE FROM THE NEGATIVE GRADIENT OF THE POTENTIAL

LLL	KLL	Z	R	V	VZ	VR	VZZ	VZR	VRR
1	1	.504	0.	-4.10660E+01	8.15100E+01	0.	5.40320E-01	0.	-2.70160E-01
1	2	1.512	0.	-1.23667E+02	8.24956E+01	0.	1.47862E+00	0.	-7.39309E-01
1	3	2.520	0.	-2.07710E+02	8.44308E+01	0.	2.51641E+00	0.	-1.25820E+00
1	4	3.528	0.	-2.94198E+02	8.74113E+01	0.	3.63736E+00	0.	-1.81868E+00
1	5	4.535	0.	-3.84205E+02	9.15379E+01	0.	4.88607E+00	0.	-2.44304E+00
1	6	5.542	0.	-4.78910E+02	9.69595E+01	0.	6.32123E+00	0.	-3.16061E+00
1	7	6.546	0.	-5.79627E+02	1.03888E+02	0.	8.02315E+00	0.	-4.01157E+00
1	8	7.547	0.	-6.87830E+02	1.12621E+02	0.	1.01078E+01	0.	-5.05391E+00
1	9	8.543	0.	-8.05170E+02	1.23473E+02	0.	1.25980E+01	0.	-6.29901E+00
1	10	9.527	0.	-9.33276E+02	1.37376E+02	0.	1.62445E+01	0.	-8.12225E+00
1	11	10.533	0.	-9.61363E+02	-7.46373E+01	0.	-9.27300E+00	0.	4.63650E+00
1	12	11.560	0.	-8.79856E+02	-8.39528E+01	0.	-9.34821E+00	0.	4.67410E+00
1	13	12.575	0.	-7.89890E+02	-9.33499E+01	0.	-9.76217E+00	0.	4.88108E+00
1	14	13.583	0.	-6.90954E+02	-1.02923E+02	0.	-9.89462E+00	0.	4.94731E+00
1	15	14.585	0.	-5.82962E+02	-1.12512E+02	0.	-9.86678E+00	0.	4.93339E+00
1	16	15.583	0.	-4.65977E+02	-1.21559E+02	0.	-9.67233E+00	0.	4.83616E+00
1	17	16.576	0.	-3.40242E+02	-1.31105E+02	0.	-9.31069E+00	0.	4.65535E+00
1	18	17.566	0.	-2.06165E+02	-1.39794E+02	0.	-8.78924E+00	0.	4.39462E+00
1	19	18.552	0.	-6.42961E+01	-1.47889E+02	0.	-8.13378E+00	0.	4.06689E+00
1	20	19.534	0.	8.47181E+01	-1.55302E+02	0.	-7.41836E+00	0.	3.70918E+00
1	21	20.514	0.	2.40317E+02	-1.62083E+02	0.	-6.83710E+00	0.	3.41855E+00
1	22	21.496	0.	4.02320E+02	-1.68978E+02	0.	-8.01081E+00	0.	4.00540E+00
1	23	22.494	0.	5.74084E+02	-1.75918E+02	0.	-9.83548E+00	0.	4.91824E+00
1	24	23.250	0.	7.04986E+02	-1.72216E+02	0.	-4.82624E-01	0.	2.41312E-01
1	25	23.875	0.	8.11545E+02	-1.65179E+02	0.	-8.61172E+00	0.	4.30586E+00
1	26	24.625	0.	9.37118E+02	-1.68289E+02	0.	-8.52292E+00	0.	4.26146E+00
1	27	25.625	0.	9.89344E+02	1.76246E+01	0.	-9.74437E-02	0.	4.87219E-02
1	28	26.875	0.	9.68151E+02	1.67463E+01	0.	-2.30168E-01	0.	1.15084E-01
1	29	28.125	0.	9.48117E+02	1.75479E+01	0.	-1.54140E-01	0.	7.70698E-02
1	30	29.375	0.	9.19505E+02	2.86957E+01	0.	1.41525E+01	0.	-7.07627E+00
1	31	30.500	0.	8.59584E+02	8.15800E+01	0.	1.71601E+01	0.	-8.58005E+00
1	32	31.500	0.	7.72722E+02	9.26577E+01	0.	3.76731E+00	0.	-1.88365E+00
1	33	32.500	0.	6.77657E+02	9.40258E+01	0.	-6.99833E-01	0.	3.49917E-01
1	34	33.500	0.	5.84083E+02	9.31707E+01	0.	-1.12117E+00	0.	5.60585E-01
1	35	34.500	0.	4.91461E+02	9.20147E+01	0.	-1.26397E+00	0.	6.31986E-01
1	36	35.500	0.	4.00048E+02	9.08217E+01	0.	-1.20446E+00	0.	6.02228E-01
1	37	36.500	0.	3.09782E+02	8.97392E+01	0.	-1.03566E+00	0.	5.17830E-01
1	38	37.500	0.	2.20506E+02	8.88567E+01	0.	-7.90800E-01	0.	3.95400E-01
1	39	38.500	0.	1.31987E+02	8.82357E+01	0.	-4.34571E-01	0.	2.47286E-01
1	40	39.500	0.	4.39430E+01	8.79066E+01	0.	-1.82410E-01	0.	9.12052E-02

LLL	KLL	Z	R	V	VZ	VR	VZZ	VZR	VRR
1	1	.504	.500	-4.10327E+01	8.14515E+01	-1.31594E-01	5.12429E-01	-2.34074E-01	-2.49242E-01
1	2	1.512	.500	-1.23575E+02	8.24252E+01	-3.67816E-01	1.46391E+00	-2.65458E-01	-7.28275E-01
1	3	2.520	.500	-2.07553E+02	8.43602E+01	-6.25977E-01	2.49141E+00	-2.82458E-01	-1.23946E+00
1	4	3.528	.500	-2.93971E+02	8.73338E+01	-9.04830E-01	3.60128E+00	-3.09930E-01	-1.79162E+00
1	5	4.535	.500	-3.83900E+02	9.14502E+01	-1.21545E+00	4.83755E+00	-3.50681E-01	-2.40664E+00
1	6	5.542	.500	-4.78516E+02	9.68572E+01	-1.57241E+00	6.25808E+00	-4.09329E-01	-3.11325E+00
1	7	6.546	.500	-5.79127E+02	1.03765E+02	-1.99575E+00	7.94289E+00	-4.92478E-01	-3.95138E+00
.	.	.	.	.	.	.	.	.	.
.	.	.	.	.	.	.	.	.	.
.	.	.	.	.	.	.	.	.	.
18	4	4.323	17.500	-1.58936E+02	3.64199E+01	-1.34309E+01	-2.00504E-01	-3.71146E+00	9.67986E-01
18	5	5.594	17.500	-2.05515E+02	3.62352E+01	-1.79656E+01	-2.98277E-01	-4.11772E+00	1.32488E+00
18	6	6.896	17.500	-2.53024E+02	3.59039E+01	-2.30994E+01	-4.56032E-01	-4.66324E+00	1.77600E+00
18	7	8.241	17.500	-3.01675E+02	3.52358E+01	-2.90583E+01	-7.70012E-01	-5.36162E+00	2.43049E+00
18	8	9.648	17.500	-3.51716E+02	3.37830E+01	-3.63659E+01	-1.63793E+00	-5.73253E+00	3.69879E+00
18	9	11.148	17.500	-4.02169E+02	3.47323E+01	-4.43594E+01	2.06644E+00	-6.91720E+00	4.68387E-01
18	10	13.051	17.500	-4.71806E+02	3.87113E+01	-6.33635E+01	3.22583E+00	-1.90008E+01	3.94934E-01
18	11	15.050	17.500	-5.61163E+02	2.95873E+01	-1.07781E+02	-6.77850E+00	-2.50467E+01	1.29374E+01
18	12	16.455	17.500	-5.95005E+02	-7.11409E+00	-1.37958E+02	-2.50431E+01	-1.64878E+01	3.29265E+01
18	13	17.371	17.500	-5.87631E+02	-7.52133E+01	-1.63807E+02	-5.12059E+01	3.21452E+01	6.05663E+01
18	14	18.072	17.500	-5.28071E+02	-1.19748E+02	-1.43175E+02	-5.01401E+01	7.65710E+01	5.83215E+01
18	15	18.682	17.500	-4.45085E+02	-1.39880E+02	-1.08232E+02	-2.91341E+01	8.99336E+01	3.53188E+01
18	16	19.257	17.500	-3.55378E+02	-1.47568E+02	-7.50552E+01	-8.77152E+00	7.87747E+01	1.30604E+01
18	17	19.827	17.500	-2.65261E+02	-1.49395E+02	-4.68037E+01	2.63091E+00	6.22012E+01	4.35815E-02
18	18	20.405	17.500	-1.75938E+02	-1.48012E+02	-2.27274E+01	7.32742E+00	4.90196E+01	-6.02871E+00
18	19	20.996	17.500	-8.74268E+01	-1.44935E+02	-1.47035E+00	8.84632E+00	4.04998E+01	-8.76230E+00
18	20	21.604	17.500	3.16380E-01	-1.40918E+02	1.83000E+01	9.45935E+00	3.57827E+01	-1.05051E+01
18	21	22.230	17.500	8.71327E+01	-1.35961E+02	3.77571E+01	1.05863E+01	3.39101E+01	-1.27438E+01
18	22	22.875	17.500	1.72449E+02	-1.29260E+02	5.78543E+01	1.35082E+01	3.40136E+01	-1.68141E+01
18	23	23.542	17.500	2.54852E+02	-1.18947E+02	7.90813E+01	1.97495E+01	3.44634E+01	-2.42685E+01
18	24	24.238	17.500	3.31342E+02	-1.02175E+02	1.00653E+02	2.98287E+01	3.02363E+01	-3.55803E+01
18	25	24.973	17.500	3.98705E+02	-7.99240E+01	1.21013E+02	3.93500E+01	1.92622E+01	-4.62651E+01
18	26	25.767	17.500	4.47851E+02	-5.14961E+01	1.28507E+02	3.19709E+01	-2.92030E+00	-3.93141E+01
18	27	26.635	17.500	4.80434E+02	-2.78903E+01	1.23807E+02	2.54412E+01	-5.37346E+00	-3.25159E+01
18	28	27.571	17.500	4.94715E+02	-6.25120E+00	1.16287E+02	1.95994E+01	-9.26491E+00	-2.62444E+01
18	29	28.551	17.500	4.91399E+02	1.14301E+01	1.06398E+02	1.65241E+01	-9.76492E+00	-2.26040E+01
18	30	29.553	17.500	4.71414E+02	2.65376E+01	9.50484E+01	1.32354E+01	-1.29234E+01	-1.86667E+01
18	31	30.559	17.500	4.37757E+02	3.78011E+01	8.09513E+01	8.75687E+00	-1.51238E+01	-1.33827E+01
18	32	31.559	17.500	3.94982E+02	4.47445E+01	6.55107E+01	3.65494E+00	-1.55735E+01	-7.39840E+00
18	33	32.556	17.500	3.48199E+02	4.74938E+01	5.14138E+01	4.72835E-01	-1.25648E+01	-3.41076E+00
18	34	33.550	17.500	3.00439E+02	4.80620E+01	4.04735E+01	-6.40646E-01	-1.00669E+01	-1.67213E+00
18	35	34.543	17.500	2.52788E+02	4.76642E+01	3.16714E+01	-8.45877E-01	-8.14219E+00	-9.63917E-01
18	36	35.535	17.500	2.05712E+02	4.70497E+01	2.43961E+01	-7.95380E-01	-6.87305E+00	-5.98683E-01
18	37	36.527	17.500	1.59264E+02	4.64621E+01	1.81346E+01	-6.57549E-01	-6.01869E+00	-3.78713E-01
18	38	37.519	17.500	1.13353E+02	4.59909E+01	1.25482E+01	-4.92913E-01	-5.46146E+00	-2.24128E-01
18	39	38.512	17.500	6.78385E+01	4.56681E+01	7.39318E+00	-3.22628E-01	-5.12353E+00	-9.98392E-02
18	40	39.504	17.500	2.29270E+01	4.44860E+01	3.34122E+00	-3.15171E+00	-1.61914E+00	2.96078E+00

LLL	KLL	Z	R	V	VZ	VR	VZZ	VZR	VRR
30	1	.504	29.500	-8.77877E+00	1.74473E+01	1.25974E-02	-2.57226E-01	-1.94305E-01	2.56796E-01
30	2	1.513	29.500	-2.62569E+01	1.71240E+01	-1.67078E-01	-3.67770E-01	-1.80928E-01	3.73434E-01
30	3	2.522	29.500	-4.33666E+01	1.66515E+01	-2.79417E-01	-6.15092E-01	-1.83211E-01	6.24563E-01
30	4	3.531	29.500	-5.98817E+01	1.59359E+01	-3.93032E-01	-8.65301E-01	-1.86289E-01	8.78624E-01
30	5	4.540	29.500	-7.55601E+01	1.49864E+01	-5.08102E-01	-1.11887E+00	-1.89705E-01	1.13610E+00
30	6	5.549	29.500	-9.01561E+01	1.37880E+01	-6.24438E-01	-1.37552E+00	-1.92773E-01	1.39668E+00
30	7	6.558	29.500	-1.03421E+02	1.23426E+01	-7.41333E-01	-1.63386E+00	-1.94525E-01	1.65899E+00
30	8	7.566	29.500	-1.15105E+02	1.06503E+01	-8.57375E-01	-1.89104E+00	-1.93653E-01	1.92011E+00
30	9	8.575	29.500	-1.24958E+02	8.71488E+00	-9.70251E-01	-2.14228E+00	-1.88450E-01	2.17517E+00
30	10	9.583	29.500	-1.32739E+02	6.54582E+00	-1.07654E+00	-2.38039E+00	-1.76856E-01	2.41688E+00
30	11	10.590	29.500	-1.38218E+02	4.16092E+00	-1.17160E+00	-2.59540E+00	-1.56537E-01	2.63511E+00
30	12	11.597	29.500	-1.41190E+02	1.58880E+00	-1.24951E+00	-2.77441E+00	-1.25155E-01	2.81676E+00
30	13	12.603	29.500	-1.41488E+02	-1.12851E+00	-1.30330E+00	-2.90186E+00	-8.08000E-02	2.94604E+00
30	14	13.607	29.500	-1.38995E+02	-3.93362E+00	-1.32540E+00	-2.96049E+00	-2.25870E-02	3.00542E+00
30	15	14.609	29.500	-1.33663E+02	-6.75308E+00	-1.30848E+00	-2.93300E+00	4.87078E-02	2.97735E+00
30	16	15.610	29.500	-1.25526E+02	-9.49864E+00	-1.24648E+00	-2.80455E+00	1.30166E-01	2.84680E+00
30	17	16.609	29.500	-1.14713E+02	-1.20708E+01	-1.13575E+00	-2.56555E+00	2.16645E-01	2.60405E+00
30	18	17.606	29.500	-1.01457E+02	-1.43649E+01	-9.76099E-01	-2.21427E+00	3.01248E-01	2.24736E+00
30	19	18.602	29.500	-8.60935E+01	-1.62790E+01	-7.71373E-01	-1.75844E+00	3.76315E-01	1.78459E+00
30	20	19.596	29.500	-6.90522E+01	-1.77226E+01	-5.29434E-01	-1.21548E+00	4.34697E-01	1.23343E+00
30	21	20.589	29.500	-5.08420E+01	-1.86251E+01	-2.61544E-01	-6.11084E-01	4.70934E-01	6.19949E-01
30	22	21.581	29.500	-3.20273E+01	-1.89423E+01	1.87844E-02	2.34646E-02	4.82037E-01	-2.41013E-02
30	23	22.573	29.500	-1.32002E+01	-1.86601E+01	2.97173E-01	6.54674E-01	4.67728E-01	-6.64747E-01
30	24	23.565	29.500	5.04920E+00	-1.77952E+01	5.59772E-01	1.25024E+00	4.30183E-01	-1.26922E+00
30	25	24.556	29.500	2.21614E+01	-1.63927E+01	7.94446E-01	1.78197E+00	3.73463E-01	-1.80890E+00
30	26	25.549	29.500	3.76337E+01	-1.45221E+01	9.91629E-01	2.22781E+00	3.02799E-01	-2.26142E+00
30	27	26.541	29.500	5.10406E+01	-1.22704E+01	1.14481E+00	2.57300E+00	2.23876E-01	-2.61180E+00
30	28	27.535	29.500	6.20481E+01	-9.73575E+00	1.25067E+00	2.81029E+00	1.42210E-01	-2.85269E+00
30	29	28.529	29.500	7.04225E+01	-7.02029E+00	1.32887E+00	2.93942E+00	6.26528E-02	-2.98379E+00
30	30	29.524	29.500	7.60311E+01	-4.22431E+00	1.32165E+00	2.96593E+00	-1.09401E-02	-3.01073E+00
30	31	30.520	29.500	7.88388E+01	-1.44118E+00	1.29323E+00	2.89978E+00	-7.58818E-02	-2.94362E+00
30	32	31.515	29.500	7.88992E+01	1.24616E+00	1.22909E+00	2.75370E+00	-1.30672E-01	-2.79537E+00
30	33	32.513	29.500	7.63438E+01	3.76728E+00	1.13534E+00	2.54170E+00	-1.74890E-01	-2.58019E+00
30	34	33.510	29.500	7.13685E+01	6.06453E+00	1.01814E+00	2.27771E+00	-2.09001E-01	-2.31222E+00
30	35	34.508	29.500	6.42204E+01	8.09456E+00	8.83178E-01	1.97456E+00	-2.34105E-01	-2.00450E+00
30	36	35.505	29.500	5.51860E+01	9.82310E+00	7.35423E-01	1.64335E+00	-2.51676E-01	-1.66828E+00
30	37	36.505	29.500	4.45797E+01	1.12272E+01	5.78902E-01	1.29306E+00	-2.63312E-01	-1.31268E+00
30	38	37.503	29.500	3.27354E+01	1.22910E+01	4.16736E-01	9.30541E-01	-2.70526E-01	-9.44667E-01
30	39	38.502	29.500	1.99996E+01	1.30049E+01	2.51198E-01	5.60787E-01	-2.74581E-01	-5.69302E-01
30	40	39.501	29.500	6.70654E+00	1.34945E+01	-1.84850E-02	3.90272E-01	-2.98457E-01	-3.89646E-01

TOTAL EDIT TIME IS 8.684 SECONDS *** *** ***

SAMPLE CASE USING VARIOUS FEATURE OF JASON

VPLOT

PLOTTING 25 LINES

-1.00000E+03
-9.16667E+02
-8.33333E+02
-7.50000E+02
-6.66667E+02
-5.83333E+02
-5.00000E+02
-4.16667E+02
-3.33333E+02
-2.50000E+02
-1.66667E+02
-8.33333E+01
-3.63798E-12
8.33333E+01
1.66667E+02
2.50000E+02
3.33333E+02
4.16667E+02
5.00000E+02
5.83333E+02
6.66667E+02
7.50000E+02
8.33333E+02
9.16667E+02
1.00000E+03

APPENDIX G

COMPARISON OF COMPUTED SOLUTION WITH ANALYTIC SOLUTION

10 CM. RADIUS SPHERICAL CHARGE DISTRIBUTION (RHO/EPS0 = 100.)

L	K	Z	R	V ERROR (%)
1	1	0.	0.	6.66667E+02 5.45697E-13
1	2	1.429	0.	6.86268E+02 9.88009E-04
1	3	2.857	0.	7.06974E+02 1.37286E-02
1	4	4.286	0.	7.28975E+02 2.63049E-02
1	5	5.714	0.	7.52396E+02 3.87784E-02
1	6	7.143	0.	7.77382E+02 5.08625E-02
1	7	8.571	0.	8.04095E+02 6.25277E-02
1	8	10.000	0.	8.32718E+02 7.37842E-02
1	9	11.429	0.	8.63466E+02 8.46663E-02
1	10	12.857	0.	8.96581E+02 9.52198E-02
1	11	14.286	0.	9.32349E+02 1.05498E-01
1	12	15.714	0.	9.71099E+02 1.15565E-01
1	13	17.143	0.	1.01322E+03 1.25497E-01
1	14	18.571	0.	1.05917E+03 1.35391E-01
1	15	20.000	0.	1.10950E+03 1.45372E-01
1	16	21.429	0.	1.16485E+03 1.55606E-01
1	17	22.857	0.	1.22603E+03 1.66297E-01
1	18	24.286	0.	1.29399E+03 1.77677E-01
1	19	25.714	0.	1.36994E+03 1.89936E-01
1	20	27.143	0.	1.45537E+03 2.03090E-01
1	21	28.571	0.	1.55218E+03 2.16716E-01
1	22	30.000	0.	1.66284E+03 2.29505E-01
1	23	31.250	0.	1.77368E+03 2.30275E-01
1	24	32.500	0.	1.90045E+03 2.26551E-01
1	25	33.750	0.	2.04684E+03 2.16562E-01
1	26	35.000	0.	2.21784E+03 1.96992E-01
1	27	36.250	0.	2.42024E+03 1.65003E-01
1	28	37.500	0.	2.66335E+03 1.24363E-01
1	29	38.750	0.	2.96000E+03 9.99685E-02
1	30	40.000	0.	3.33004E+03 9.87726E-02
1	31	41.000	0.	3.64673E+03 9.05030E-02
1	32	42.000	0.	3.93019E+03 7.99743E-02
1	33	43.000	0.	4.18074E+03 6.19654E-02
1	34	44.000	0.	4.39809E+03 4.34765E-02
1	35	45.000	0.	4.58203E+03 2.84847E-02
1	36	46.000	0.	4.73248E+03 1.80023E-02
1	37	47.000	0.	4.84945E+03 1.13896E-02
1	38	48.000	0.	4.93296E+03 7.57939E-03
1	39	49.000	0.	4.98305E+03 5.68527E-03
1	40	50.000	0.	4.99974E+03 5.11675E-03
.	.	.	.	.
.	.	.	.	.
.	.	.	.	.
3	1	0.	2.564	6.65792E+02 2.18566E-12
3	2	1.424	2.550	6.85170E+02 1.45444E-02
3	3	2.849	2.536	7.05721E+02 2.85652E-02

L	K	Z	R	V ERROR (%)
2	1	0.	1.282	6.66448E+02 5.45876E-13
2	2	1.426	1.275	6.85923E+02 1.23904E-02
2	3	2.853	1.268	7.06573E+02 2.52823E-02
2	4	4.279	1.261	7.28508E+02 3.86657E-02
2	5	5.706	1.254	7.51859E+02 5.18075E-02
2	6	7.133	1.246	7.76768E+02 6.46079E-02
2	7	8.560	1.238	8.03397E+02 7.70421E-02
2	8	9.987	1.230	8.31931E+02 8.91341E-02
2	9	11.415	1.221	8.62581E+02 1.00927E-01
2	10	12.842	1.211	8.95594E+02 1.12473E-01
2	11	14.270	1.200	9.31251E+02 1.23835E-01
2	12	15.699	1.188	9.69885E+02 1.35084E-01
2	13	17.127	1.176	1.01189E+03 1.46304E-01
2	14	18.556	1.162	1.05771E+03 1.57601E-01
2	15	19.986	1.146	1.10791E+03 1.69110E-01
2	16	21.416	1.129	1.16313E+03 1.81010E-01
2	17	22.846	1.111	1.22417E+03 1.93526E-01
2	18	24.276	1.090	1.29199E+03 2.06923E-01
2	19	25.707	1.069	1.36779E+03 2.21458E-01
2	20	27.138	1.046	1.45305E+03 2.37247E-01
2	21	28.569	1.023	1.54967E+03 2.54046E-01
2	22	30.000	1.000	1.66008E+03 2.70814E-01
2	23	31.251	.997	1.77046E+03 2.77155E-01
2	24	32.503	.993	1.89670E+03 2.80518E-01
2	25	33.757	.984	2.04264E+03 2.79396E-01
2	26	35.013	.969	2.21351E+03 2.70632E-01
2	27	36.273	.943	2.41656E+03 2.49887E-01
2	28	37.537	.905	2.66179E+03 2.18115E-01
2	29	38.799	.851	2.96180E+03 1.91566E-01
2	30	40.031	.786	3.32691E+03 1.93237E-01
2	31	41.049	.828	3.66605E+03 2.00797E-01
2	32	42.038	.876	3.92299E+03 1.92730E-01
2	33	43.021	.920	4.16673E+03 1.76121E-01
2	34	44.008	.953	4.37953E+03 1.58255E-01
2	35	45.001	.976	4.56105E+03 1.43326E-01
2	36	45.998	.990	4.71047E+03 1.32382E-01
2	37	46.997	.997	4.82711E+03 1.24870E-01
2	38	47.998	1.000	4.91061E+03 1.20030E-01
2	39	48.999	1.001	4.96078E+03 1.17267E-01
2	40	50.000	1.000	4.97754E+03 1.16264E-01
.	.	.	.	.
.	.	.	.	.
.	.	.	.	.
4	1	0.	3.846	6.64703E+02 5.47309E-13
4	2	1.422	3.826	6.83960E+02 1.53699E-02
4	3	2.844	3.805	7.04377E+02 2.99577E-02

L	K	Z	R	V ERROR (%)
19	24	32.500	20.000	1.25196E+03 1.86390E-01
19	25	33.750	20.000	1.29105E+03 1.91139E-01
19	26	35.000	20.000	1.33071E+03 1.96637E-01
19	27	36.250	20.000	1.37062E+03 2.02710E-01
19	28	37.500	20.000	1.41037E+03 2.09378E-01
19	29	38.750	20.000	1.44948E+03 2.16752E-01
19	30	40.000	20.000	1.48727E+03 2.31216E-01
19	31	41.000	20.000	1.51616E+03 2.43897E-01
19	32	42.000	20.000	1.54357E+03 2.51667E-01
19	33	43.000	20.000	1.56902E+03 2.59039E-01
19	34	44.000	20.000	1.59213E+03 2.66019E-01
19	35	45.000	20.000	1.61250E+03 2.72348E-01
19	36	46.000	20.000	1.62976E+03 2.77774E-01
19	37	47.000	20.000	1.64358E+03 2.82109E-01
19	38	48.000	20.000	1.65366E+03 2.85247E-01
19	39	49.000	20.000	1.65981E+03 2.87157E-01
19	40	50.000	20.000	1.66187E+03 2.87835E-01
.	.	.	.	.
.	.	.	.	.
.	.	.	.	.
21	1	0.	25.641	5.93212E+02 3.06634E-12
21	2	1.365	25.576	6.06553E+02 8.96231E-03
21	3	2.730	25.511	6.20452E+02 1.76010E-02
21	4	4.095	25.444	6.34943E+02 2.59375E-02
21	5	5.462	25.376	6.50061E+02 3.39935E-02
21	6	6.830	25.306	6.65847E+02 4.17907E-02
21	7	8.198	25.233	6.82344E+02 4.93502E-02
21	8	9.568	25.157	6.99599E+02 5.66923E-02
21	9	10.940	25.078	7.17663E+02 6.38363E-02
21	10	12.314	24.994	7.36592E+02 7.08009E-02
21	11	13.689	24.906	7.56448E+02 7.76039E-02
.	.	.	.	.
.	.	.	.	.
.	.	.	.	.
39	18	21.856	48.645	5.93084E+02 6.57887E-03
39	19	23.140	48.640	5.99870E+02 7.02239E-03
39	20	24.424	48.635	6.06562E+02 7.47542E-03
39	21	25.707	48.631	6.13138E+02 7.93704E-03
39	22	26.991	48.627	6.19576E+02 8.40579E-03
39	23	28.273	48.622	6.25855E+02 8.87967E-03
39	24	29.555	48.618	6.31951E+02 9.35619E-03
39	25	30.837	48.614	6.37840E+02 9.83240E-03
39	26	32.118	48.610	6.43499E+02 1.03049E-02
39	27	33.399	48.606	6.48903E+02 1.07701E-02
39	28	34.679	48.603	6.54028E+02 1.12242E-02
39	29	35.958	48.599	6.58850E+02 1.16630E-02
39	30	37.237	48.596	6.63345E+02 1.20826E-02
39	31	38.515	48.593	6.67492E+02 1.24791E-02
39	32	39.793	48.590	6.71269E+02 1.28488E-02
39	33	41.070	48.588	6.74655E+02 1.31881E-02
39	34	42.347	48.585	6.77634E+02 1.34939E-02
39	35	43.623	48.583	6.80188E+02 1.37636E-02
39	36	44.899	48.580	6.82303E+02 1.39950E-02
39	37	46.174	48.578	6.83967E+02 1.41868E-02
39	38	47.450	48.576	6.85172E+02 1.43391E-02
39	39	48.725	48.574	6.85909E+02 1.44546E-02
39	40	50.000	48.571	6.86175E+02 1.45484E-02

L	K	Z	R	V ERROR (%)
20	24	32.146	21.578	1.18810E+03 1.74135E-01
20	25	33.427	21.537	1.22438E+03 1.81030E-01
20	26	34.688	21.511	1.26008E+03 1.87926E-01
20	27	35.936	21.493	1.29523E+03 1.95263E-01
20	28	37.171	21.480	1.32958E+03 2.03381E-01
20	29	38.387	21.470	1.36267E+03 2.12704E-01
20	30	39.574	21.463	1.39388E+03 2.21112E-01
20	31	40.685	21.457	1.42180E+03 2.24420E-01
20	32	41.754	21.452	1.44699E+03 2.33358E-01
20	33	42.803	21.448	1.46984E+03 2.41445E-01
20	34	43.842	21.445	1.49029E+03 2.48609E-01
20	35	44.874	21.441	1.50816E+03 2.54861E-01
20	36	45.903	21.439	1.52322E+03 2.60132E-01
20	37	46.929	21.436	1.53524E+03 2.64325E-01
20	38	47.953	21.433	1.54403E+03 2.67350E-01
20	39	48.977	21.431	1.54943E+03 2.69122E-01
20	40	50.000	21.429	1.55136E+03 2.69512E-01
.	.	.	.	.
.	.	.	.	.
.	.	.	.	.
22	1	0.	26.923	5.86981E+02 6.19778E-13
22	2	1.360	26.860	5.99863E+02 8.38015E-03
22	3	2.720	26.796	6.13261E+02 1.64721E-02
22	4	4.082	26.732	6.27207E+02 2.42930E-02
22	5	5.443	26.666	6.41730E+02 3.18606E-02
22	6	6.806	26.598	6.56864E+02 3.91928E-02
22	7	8.170	26.528	6.72647E+02 4.63076E-02
22	8	9.535	26.454	6.89116E+02 5.32224E-02
22	9	10.901	26.378	7.06314E+02 5.99543E-02
22	10	12.269	26.298	7.24285E+02 6.65199E-02
22	11	13.638	26.214	7.43078E+02 7.29354E-02
.	.	.	.	.
.	.	.	.	.
.	.	.	.	.
40	18	21.795	50.000	5.80652E+02 6.26533E-13
40	19	23.077	50.000	5.86981E+02 3.09889E-12
40	20	24.359	50.000	5.93212E+02 1.83980E-12
40	21	25.641	50.000	5.99327E+02 1.82103E-12
40	22	26.923	50.000	6.05306E+02 2.40406E-12
40	23	28.205	50.000	6.11131E+02 1.19057E-12
40	24	29.487	50.000	6.16779E+02 1.17967E-12
40	25	30.769	50.000	6.22230E+02 3.50800E-12
40	26	32.051	50.000	6.27463E+02 2.89896E-12
40	27	33.333	50.000	6.32456E+02 5.75215E-13
40	28	34.615	50.000	6.37186E+02 1.71283E-12
40	29	35.897	50.000	6.41633E+02 3.40192E-12
40	30	37.179	50.000	6.45776E+02 1.12670E-12
40	31	38.462	50.000	6.49594E+02 2.24015E-12
40	32	39.744	50.000	6.53068E+02 2.78530E-12
40	33	41.026	50.000	6.56181E+02 5.54417E-13
40	34	42.308	50.000	6.58914E+02 2.76059E-12
40	35	43.590	50.000	6.61254E+02 2.20065E-12
40	36	44.872	50.000	6.63188E+02 2.19424E-12
40	37	46.154	50.000	6.64703E+02 2.73654E-12
40	38	47.436	50.000	6.65792E+02 1.63924E-12
40	39	48.718	50.000	6.66448E+02 5.45876E-13
40	40	50.000	50.000	6.66667E+02 5.45697E-13

FIGURE LEGEND

Fig. 1 Sample problem geometry.

Fig. 2 Logical diagram for sample problem.

Fig. 3 Alternate zoning for grid A of sample problem.

Fig. 4 Mesh plot for sample problem.

Fig. 5 Equipotential plot for sample problem.

Fig. 6 Equipotential plot for a spherical charge distribution.

Fig. 7 Equipotential plot for a dielectric sphere in a uniform field.

Fig. 8 Mesh plot for eletrostatic quadrupole.

Fig. 9 Equipotential plot for electrostratic quadrupole.

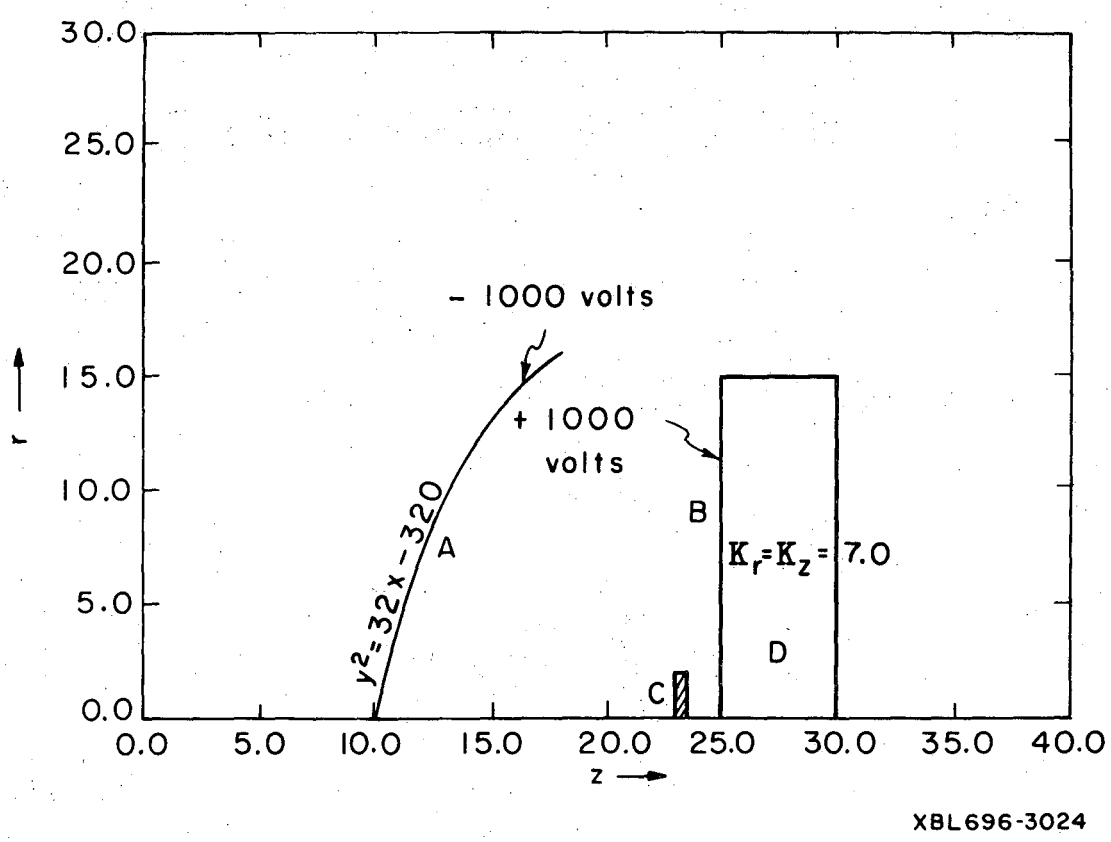
30.0
25.0
20.0
15.0
10.0
5.0
0.0
r
- 1000 volts
+ 1000 volts
$y^2 = 32x - 320$
A
B
C
D
$K_r = K_z = 7.0$
0.0
5.0
10.0
15.0
20.0
25.0
30.0
35.0
40.0
z
XBL696-3024

Fig. 1

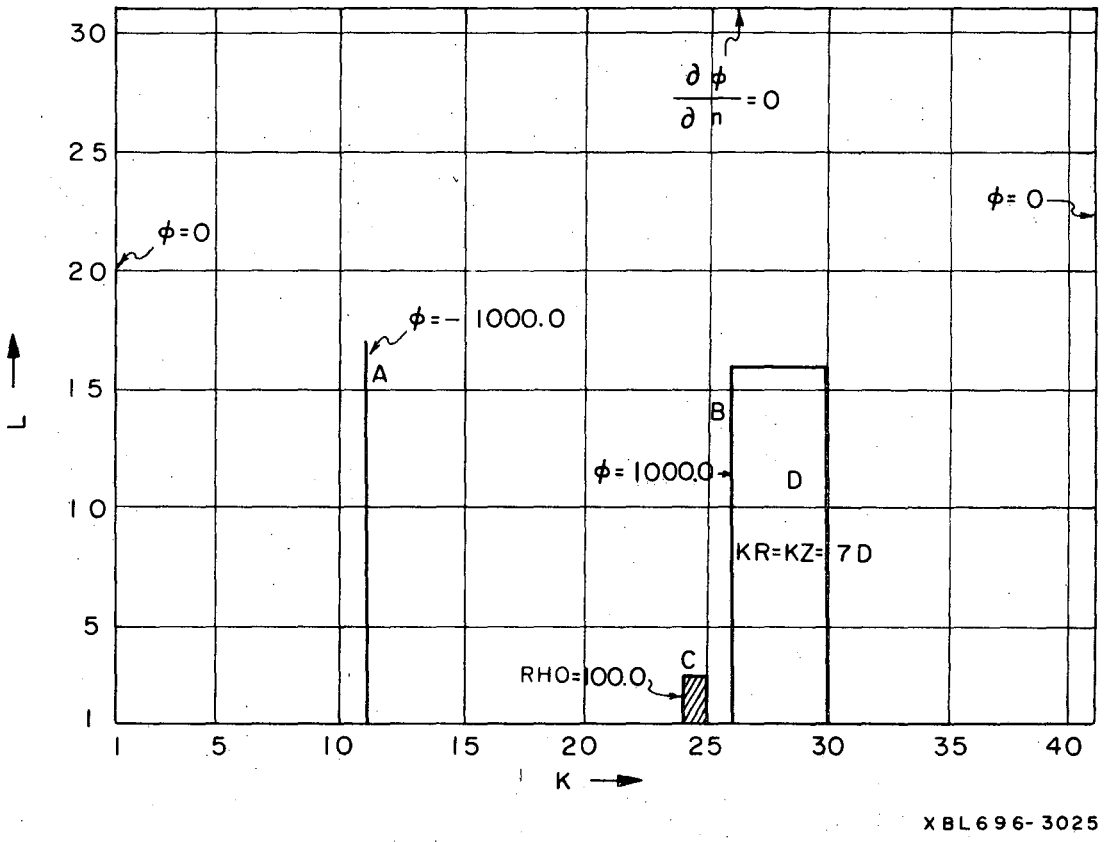
30
25
20
15
10
5
1
1
5
10
15
20
25
30
35
40
J
K
∂φ/∂n = 0
φ = 0
φ = 0
φ = − 1000.0
A
B
φ = 1000.0
D
KR=KZ= 7D
C
RHO=100.0
XBL696-3025

Fig. 2

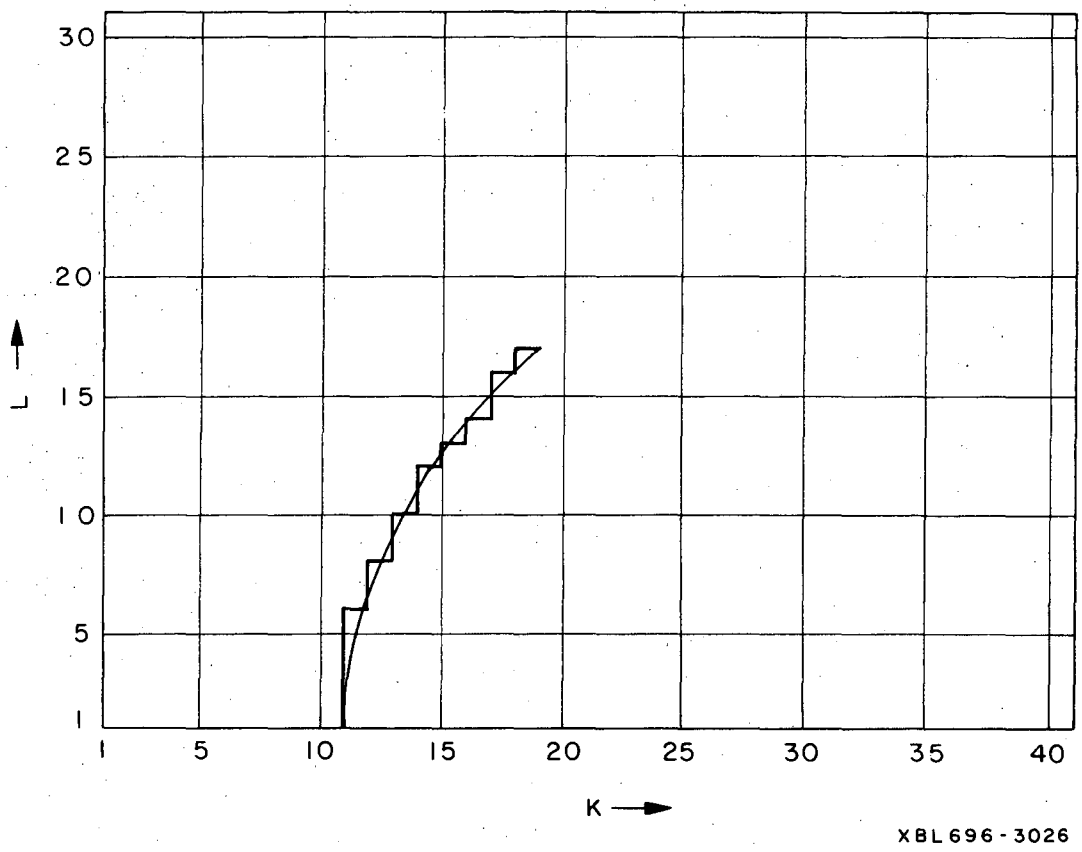

Fig. 3

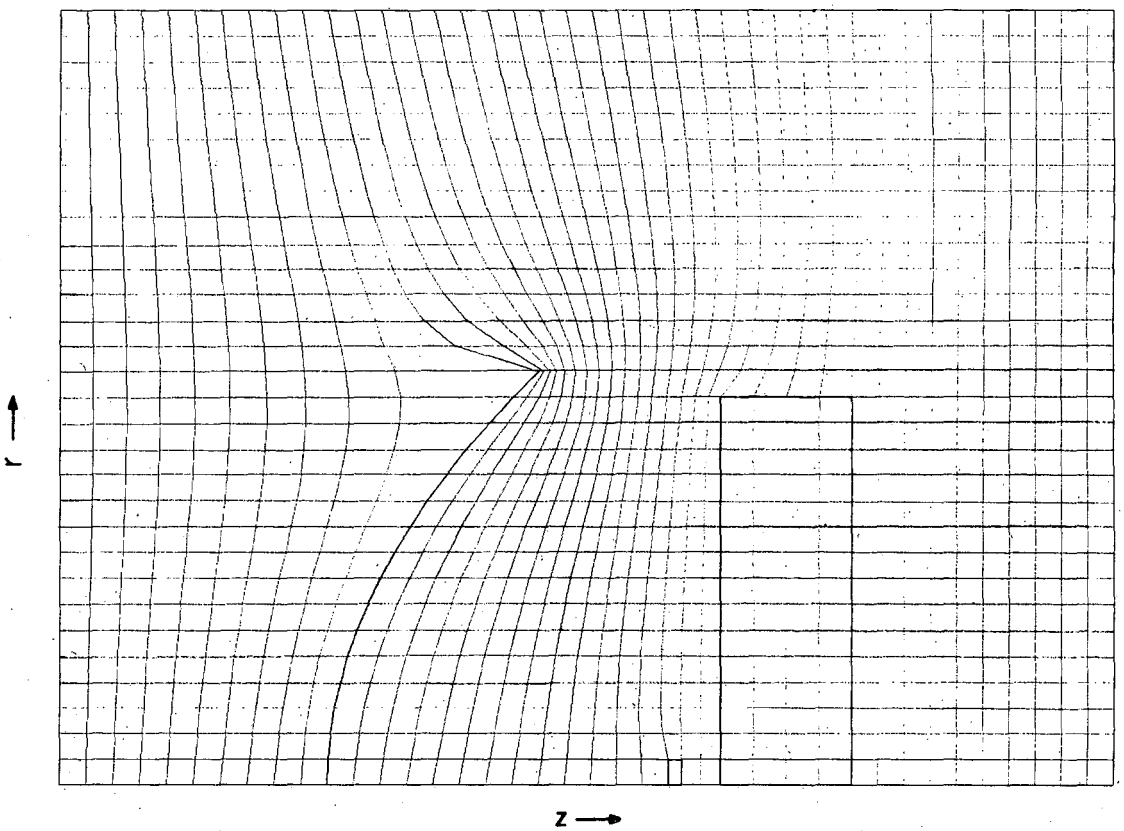

XBL696-3027

Fig. 4

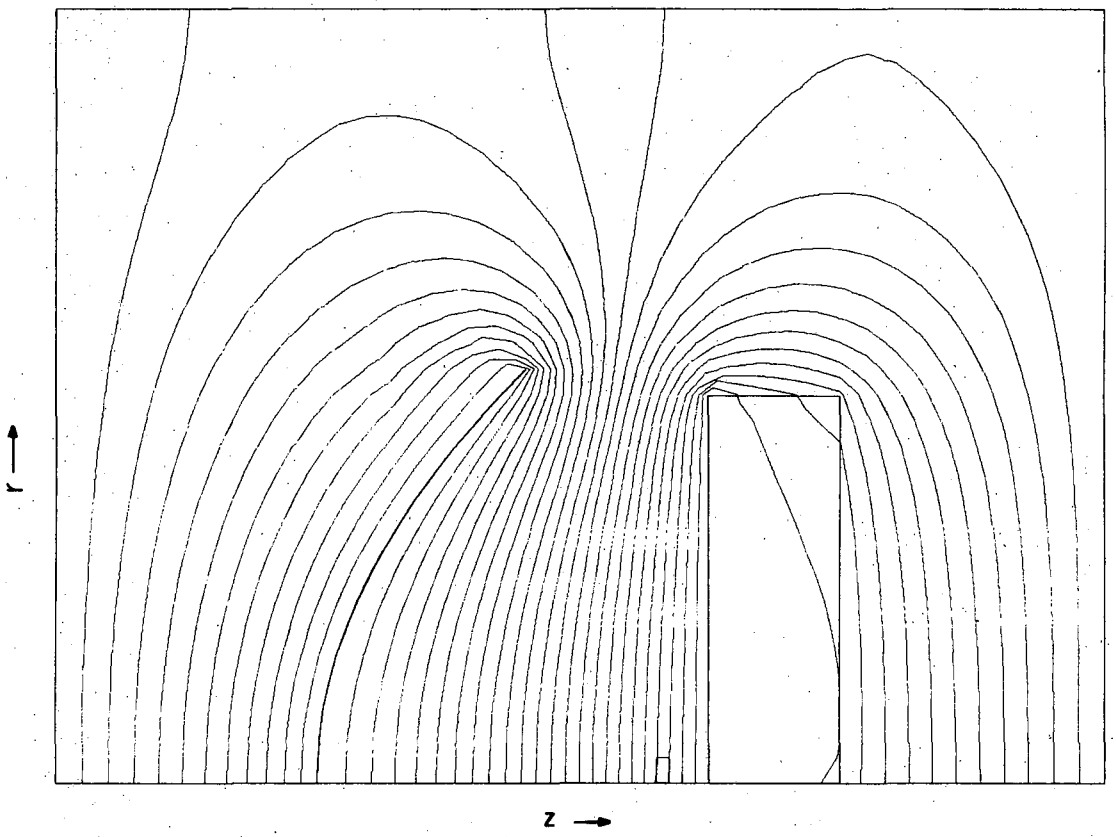

Fig. 5

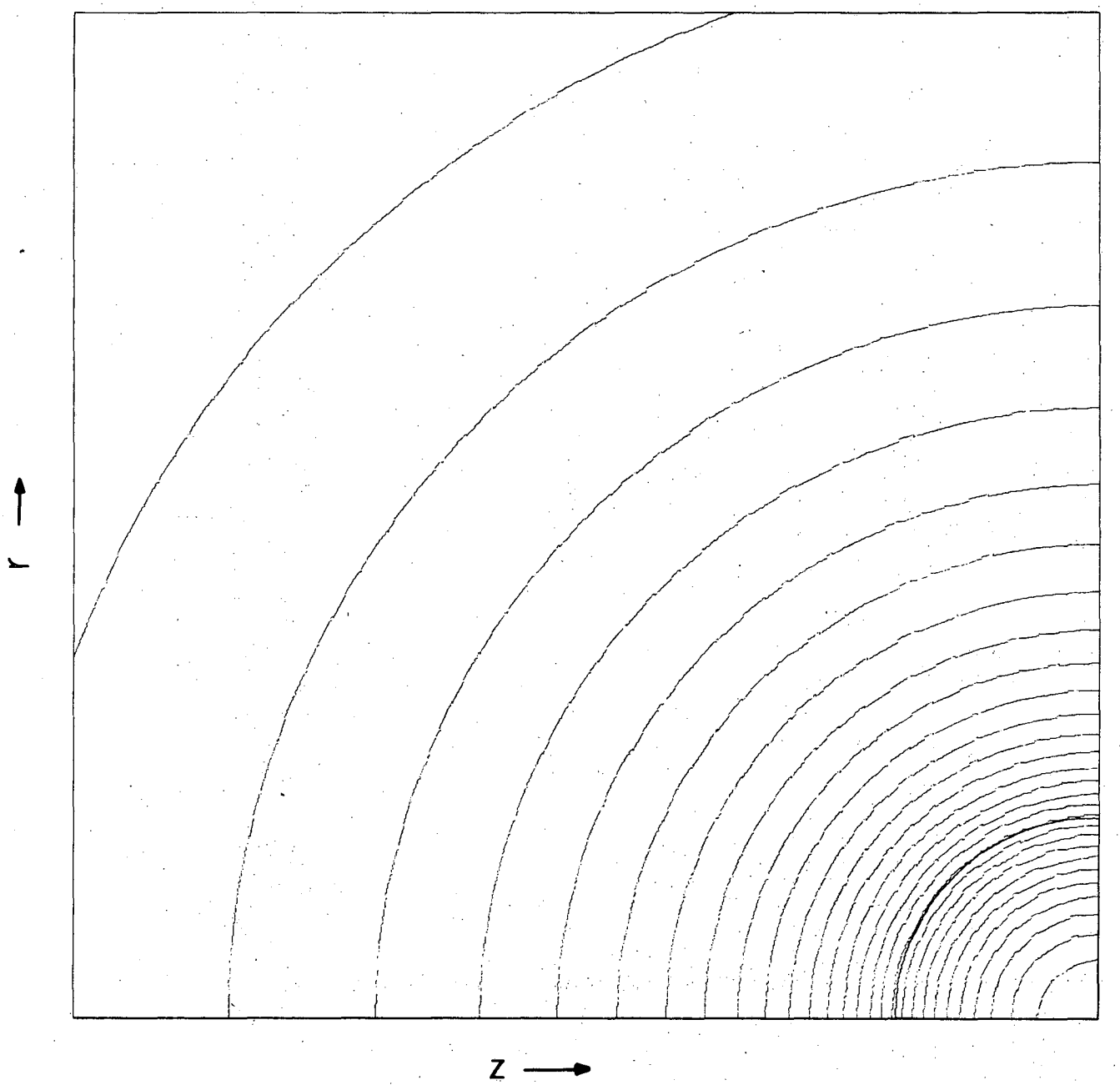

XBL696-3029

Fig. 6

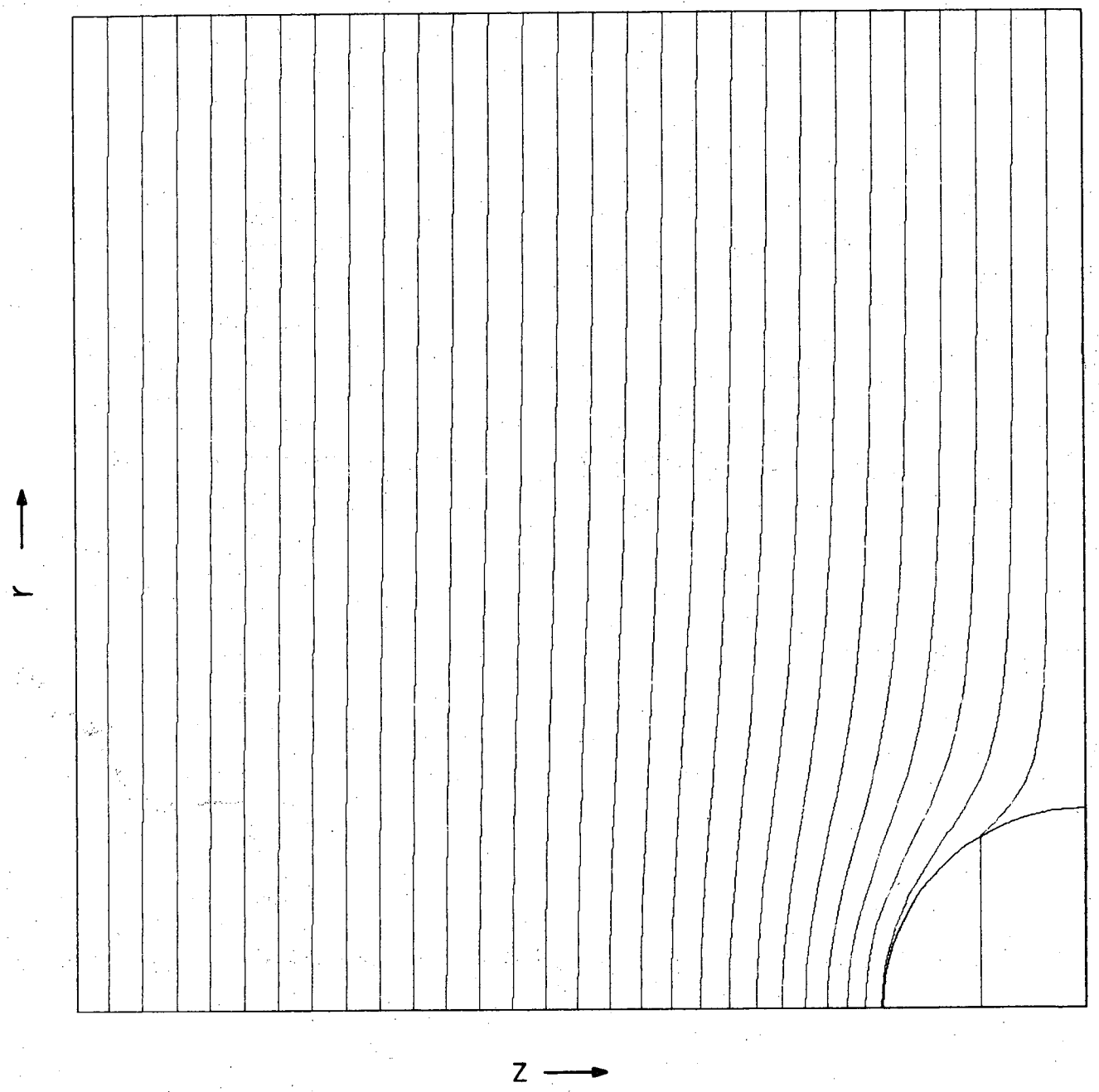

XBL696 - 3030

Fig. 7

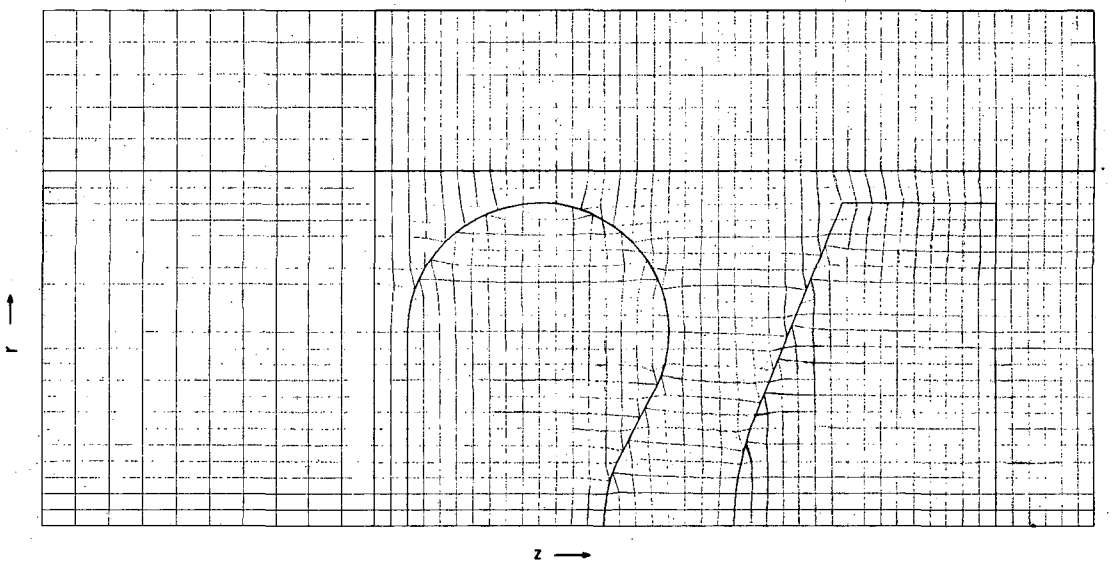

Fig. 8

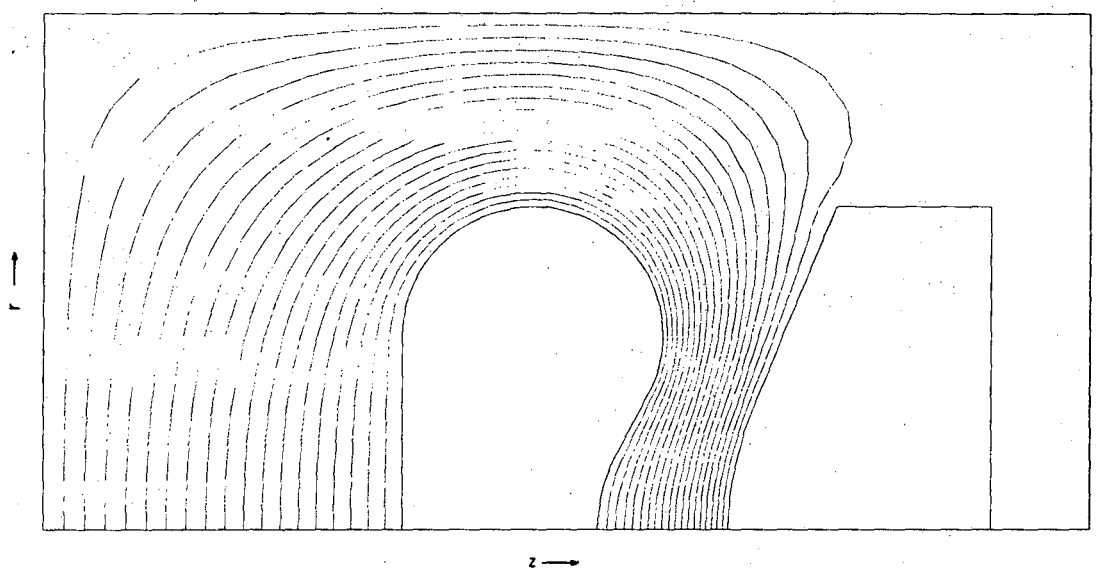

XBL696-3032

Fig. 9

TECHNICAL INFORMATION DIVISION
LAWRENCE RADIATION LABORATORY
UNIVERSITY OF CALIFORNIA
BERKELEY, CALIFORNIA 94720